

Phase Retrieval of Quaternion Signal via Wirtinger Flow

Junren Chen*

Michael K. Ng[†]

Abstract

The main aim of this paper is to study quaternion phase retrieval (QPR), i.e., the recovery of quaternion signal from magnitude of quaternion linear measurements. We show that all d -dimensional quaternion signals can be reconstructed up to a global right quaternion phase factor from $O(d)$ phaseless measurements. We also develop the scalable algorithm quaternion Wirtinger flow (QWF) for solving QPR, and establish its linear convergence guarantee. Compared with the analysis of complex Wirtinger flow, a series of different treatments are employed to overcome the difficulties arising in the quaternion setting, especially those from the non-commutativity of quaternion multiplication. For instance, the concentration ingredients are established by using the real matrix representation of a quaternion matrix rather than the Hessian matrix of ℓ_2 loss function. Moreover, we develop a variant of QWF that can effectively utilize a pure quaternion priori (e.g., for color images) by incorporating a quaternion phase factor estimate into QWF iterations. The estimate is obtained by finding a singular vector of a 4×4 real matrix constructed from the QWF iterate, and hence can be computed efficiently. Experimental results on synthetic data and color images are presented to validate our theoretical results.

1 Introduction

As an expansion of the complex field \mathbb{C} , an element in the non-commutative field $\mathbb{Q} = \{q_0 + q_1 \mathbf{i} + q_2 \mathbf{j} + q_3 \mathbf{k} : q_0, q_1, q_2, q_3 \in \mathbb{R}\}$ is called a quaternion number, which contains one real part (q_0) and three imaginary parts (q_1, q_2, q_3). While signals or images are traditionally processed in \mathbb{R} or \mathbb{C} , the quaternion algebra has been noted to be a suitable platform for signal processing tasks. Consequently, many signal processing tools have been developed for quaternion setting over the past decades, including Fourier transform [20, 50], wavelet transform [5, 24], principal component analysis [32], moment analysis [11, 12], compressed sensing [1], matrix completion [13, 31], deep neural network [27, 69], adaptive filtering [56–58], quaternion derivative [35, 65–67], and many others.

Color image processing is one of the important applications of quaternion. Compared with monochromatic model that processes color images channel-by-channel, the quaternion-based approach encodes three channels (e.g., Red, Green and Blue in the RGB color space) into three imaginary parts of pure quaternion while the real part is set to zero. The advantage of

*Department of Mathematics, The University of Hong Kong. E-mail: chenjr58@connect.hku.hk

[†]Department of Mathematics, The University of Hong Kong. E-mail: mng@maths.hku.hk. This work is supported by Hong Kong Research Grant Council GRF 12300218, 12300519, 17201020, 17300021, C1013-21GF, C7004-21GF and Joint NSFC-RGC N-HKU76921.

quaternion-based approach is that the correlation among the three channels can be kept, and color images can be processed in a holistic manner. This approach was proposed in [20, 46, 50], and now has been extensively developed in various color imaging problems including denoising [17, 26, 29], inpainting [13, 31, 39], segmentation [52, 55], convolution neural network [45], watermarking [4, 63]. By taking advantage of holistic processing of color images, quaternion-based approach usually outperforms monochromatic model based on mathematical operations in real or complex field, see for instance [17, 26, 29, 31, 39].

Phase retrieval concerning signal reconstruction from phaseless measurements has attracted vast research interest. It is motivated by a frequently encountered setting where it would be expensive, difficult, or even impossible to capture the measurement phase, to name a few, X-ray crystallography [41], quantum mechanics [49], speech recognition [48]. We further emphasize the crucial role played by phase retrieval in many imaging problems like diffraction imaging [7], astronomical imaging [21], optics and microscopy [38, 61]. For detailed discussion, we refer to the survey paper [51].

A mathematical formulation of phase retrieval is to recover a signal $\mathbf{x} \in \mathbb{R}^d/\mathbb{C}^d$ based on the given knowledge of measurement matrix $\mathbf{A} \in \mathbb{R}^{n \times d}/\mathbb{C}^{n \times d}$ and the corresponding phaseless measurements $|\mathbf{A}\mathbf{x}|^2$ ($|\cdot|^2$ here applies element-wisely). From the theoretical side, it is possible to reconstruct all signals up to a global phase factor (i.e., a sign ± 1 in \mathbb{R} or a unit complex scalar $\exp(i\theta)$ in \mathbb{C}) under optimal sample complexity $O(d)$, see [2, 3, 18, 64] for instance. While most early algorithms for phase retrieval lack theoretical support [22, 23, 28], a series of guaranteed algorithms has been developed in the past decade, which can be divided into a convex optimization approach [10] and a non-convex optimization approach [9, 15, 44, 62]. It is well-known that the seminal work Wirtinger flow (WF) [9] provides a framework for algorithmic design under a non-convex optimization setting, i.e., via a careful initialization that can well approximate the solution, followed by gradient descent refinement. In many cases, this is essentially more practical and scalable than a convex lifting approach [10].

Although quaternion is widely used to represent and process color images, and phase retrieval is a crucial technique in imaging science problems, quaternion phase retrieval (QPR) has not yet been studied before. More precisely, given a quaternion measurement matrix $\mathbf{A} \in \mathbb{Q}^{n \times d}$, QPR is concerned with the recovery of $\mathbf{x} \in \mathbb{Q}^d$ from the phaseless measurements $|\mathbf{A}\mathbf{x}|^2$. To our best knowledge, the only related result is presented in [16], but it is restricted to $\mathbf{A} \in \mathbb{R}^{n \times d}$. Under such real measurement matrix, the model fails to utilize the quaternion multiplication but simply identifies \mathbb{Q} as \mathbb{R}^4 , thereby reducing to a special case of phase retrieval of real vector-valued signal. More prominently, compared with $\mathbf{A} \in \mathbb{Q}^{n \times d}$ studied in this work, $\mathbf{A} \in \mathbb{R}^{n \times d}$ leads to essentially more trivial ambiguities that can probably limit applications of QPR in signal processing.

The main aim of this paper is to close the research gap between phase retrieval and quaternion signal processing. We initiate the study of QPR, by first identifying the unavoidable trivial ambiguity, and then proposing and studying a practical algorithm of quaternion Wirtinger flow (QWF) with a linear convergence guarantee. This work is built upon many previous developments of quaternion, for instance, the HR calculus of quaternion derivative [35, 66], and results for quaternion matrices [68]. As color image processing is to deal with pure quaternion, we also develop an algorithm that can incorporate the priori of a pure quaternion signal (i.e., $\Re(\mathbf{x}) = 0$) into QWF. Our main contributions are summarized as follows:

- (Trivial Ambiguity) By Mendelson’s small ball method, we show that all signals in \mathbb{Q}^d can be reconstructed up to a global right quaternion phase factor from magnitude of $O(d)$

quaternion linear measurements (Theorem 1). On the other hand, for almost all pure quaternion signals, one can expect a reconstruction up to a sign of ± 1 (Lemma 5).

- **(Quaternion Wirtinger Flow)** For solving QPR, we propose the QWF algorithm consisting of spectral initialization and QWF refinement. Our main result (Theorem 2) guarantees that under the magnitude of $O(d \log n)$ quaternion Gaussian measurements and an error metric $\text{dist}(\mathbf{x}, \mathbf{y}) = \min_{|q|=1} \|\mathbf{x} - \mathbf{y}q\|$, the QWF sequence linearly converges to the underlying signal with high probability. Moreover, we propose a variant of QWF (pure quaternion Wirtinger flow, PQWF) for pure quaternion signal recovery. In the design, PQWF embeds an efficient quaternion phase factor estimate into the iteration and enjoys similar theoretical guarantee (Theorem 3). The earlier phase transition is presented to confirm the efficacy of PQWF (Figure 2).

We would like to point out that many essentially different treatments take place in the proof of Theorem 2 to address some technical issues arising in quaternion setting. An evident example is the concentration of $\frac{1}{n} \sum_{k=1}^n [\Re(\mathbf{x}^* \boldsymbol{\alpha}_k \boldsymbol{\alpha}_k^* \mathbf{h})]^2$, where $\boldsymbol{\alpha}_k^*$ is the k -th row of \mathbf{A} . In the proof, we avoid the Hessian matrix employed in [9] (Remark 2), and instead calculate the concentration of $\frac{1}{n} \sum_{k=1}^n [\Re(\mathbf{x}^* \boldsymbol{\alpha}_k \boldsymbol{\alpha}_k^* \mathbf{h})]^2$ by using a real matrix representation $\mathcal{T}(\cdot)$ of a quaternion. The formal definition of $\mathcal{T}(\cdot)$ can be found in Section 2. Moreover, we establish a slightly more general concentration ingredient with several technical refinements (Remark 6). In our analysis, such real matrix representations are recurring, e.g., (3.16), (3.27). Actually, with a great deal of quaternion-based ingredients involved in the theoretical analysis, we believe this work can technically provide an example for quaternion study and hence of some pedagogical value.

This paper is organized as follows. In Section 2 we state the notation and provide the preliminaries. Several useful techniques for quaternion study are included. In Section 3 we first identify the trivial ambiguity in QPR, then propose QWF, and present the proof for its linear convergence. In Section 4, we propose PQWF for QPR of pure quaternion signal. Experimental results on both synthetic data and color image data are presented in Section 5. We give some remarks to conclude the paper in Section 6. To improve the readability, some auxiliary results for the main proof are provided in Appendix A.

2 Notations and Preliminaries

Some notations are needed for mathematical analysis. We denote probability and expectation respectively by $\mathbb{P}(\cdot)$ and $\mathbb{E}(\cdot)$, note that $\mathbb{E}(\cdot)$ separately operates on one real part and three imaginary parts of a quaternion random variable. Besides, C, c, C_i, c_i represent absolute constants whose value may vary from line to line. Both $T_1 \lesssim T_2$ and $T_1 = O(T_2)$ mean $T_1 \leq CT_2$ for some absolute constant C , while $T_1 \geq CT_2$ is denoted by $T_1 \gtrsim T_2$ or $T_1 = \Omega(T_2)$.

We use capital boldface letters, lowercase boldface letters, regular letters to denote matrix, vector, and scalar, respectively. We conventionally write $[m] = \{1, \dots, m\}$. Let $\mathbb{Q} = \{q = q_0 + q_1 \mathbf{i} + q_2 \mathbf{j} + q_3 \mathbf{k} : q_0, q_1, q_2, q_3 \in \mathbb{R}\}$ be the set of quaternion numbers, then \mathbb{Q}^d (resp. $\mathbb{Q}^{d_1 \times d_2}$) denotes the set of d -dimensional quaternion vectors (resp. $n_1 \times n_2$ quaternion matrices). The addition and subtraction of two quaternion numbers are defined component-wisely, e.g., $(a \mathbf{i} + b \mathbf{k}) - (c \mathbf{j} + d \mathbf{i}) = (a - d) \mathbf{i} - c \mathbf{j} + b \mathbf{k}$. Under the rules $\mathbf{i}^2 = \mathbf{j}^2 = \mathbf{k}^2 = -1$, $\mathbf{i} \mathbf{j} = -\mathbf{j} \mathbf{i} = \mathbf{k}$, $\mathbf{j} \mathbf{k} = -\mathbf{k} \mathbf{j} = \mathbf{i}$, $\mathbf{k} \mathbf{i} = -\mathbf{i} \mathbf{k} = \mathbf{j}$ and with distributive law, associative law imposed, the multiplication between quaternion numbers is defined.

Given $q = q_0 + q_1 \mathbf{i} + q_2 \mathbf{j} + q_3 \mathbf{k}$, besides the real part $\Re(q) = q_0$ and the vector part $\Im(q) = q_1 \mathbf{i} + q_2 \mathbf{j} + q_3 \mathbf{k}$, we further use \mathcal{P}^ϑ ($\vartheta = \mathbf{i}, \mathbf{j}, \mathbf{k}$) to extract three imaginary components, e.g., $\mathcal{P}^{\mathbf{i}}(q) = q_1$. Note that $\bar{q} = q_0 - q_1 \mathbf{i} - q_2 \mathbf{j} - q_3 \mathbf{k}$ is the conjugate of q , $|q| = (\sum_{k=0}^3 q_k^2)^{1/2}$ is the absolute value. We allow these operations for quaternion number element-wisely apply to quaternion vectors and matrices. For nonzero q , $q^{-1} = \bar{q}/|q|^2$ is its inverse.

Given the vector $\mathbf{x} = [x_k] \in \mathbb{Q}^d$ or the matrix $\mathbf{A} = [a_{ij}] \in \mathbb{Q}^{d_1 \times d_2}$, we introduce the (vector) ℓ_2 norm $\|\mathbf{x}\| = (\sum_k |x_k|^2)^{1/2}$, the matrix operator norm $\|\mathbf{A}\| = \sup_{\mathbf{w} \in \mathbb{Q}^{d_1} \setminus \{0\}} \|\mathbf{A}\mathbf{w}\|/\|\mathbf{w}\|$, the matrix Frobenius norm $\|\mathbf{A}\|_F = (\sum_{i,j} |a_{ij}|^2)^{1/2}$. The rank of \mathbf{A} , denoted $\text{rank}(\mathbf{A})$, is defined to be the maximum number of right linearly independent columns of \mathbf{A} . Note that quaternion vectors $\alpha_1, \dots, \alpha_N$ are said to be right linearly independent if $\sum_{k=1}^N \alpha_k q_k = 0$ ($q_k \in \mathbb{Q}$) can imply $q_k = 0$ for all k . Let \mathbf{I}_d be the identity matrix, the matrix $\mathbf{A} \in \mathbb{Q}^{d \times d}$ is invertible if there exists \mathbf{B} such that $\mathbf{A}\mathbf{B} = \mathbf{B}\mathbf{A} = \mathbf{I}_d$. Parallel to complex matrices, \mathbf{A} is invertible if and only if it is full rank ($\text{rank}(\mathbf{A}) = d$) [68]. We say $\mathbf{A} \in \mathbb{Q}^{d \times d}$ is Hermitian if $\mathbf{A}^* = \mathbf{A}$, or is unitary if $\mathbf{A}\mathbf{A}^* = \mathbf{A}^*\mathbf{A} = \mathbf{I}_d$. We use $\mathcal{H}_{d,r}^{\mathbb{Q}}$ to denote the set of all $d \times d$ Hermitian matrices with rank not exceeding r . The standard inner product for quaternion vector or matrix is given by $\langle \mathbf{A}, \mathbf{B} \rangle = \text{Tr}(\mathbf{A}^*\mathbf{B})$, where $\text{Tr}(\cdot)$ returns the sum of diagonal entries for a square matrix, or simply the scalar itself. Evidently, $\Re\langle \mathbf{A}, \mathbf{B} \rangle = \Re\langle \mathbf{B}, \mathbf{A} \rangle$.

Note that quaternion multiplication is non-commutative (e.g., $\mathbf{i}\mathbf{j} = -\mathbf{j}\mathbf{i}$), which is often a key technical challenge in the extension from \mathbb{R}/\mathbb{C} to quaternion setting. We note that, taking the real part is an effective technique to circumvent this issue, since we have $\Re(ab) = \Re(ba)$ for any $a, b \in \mathbb{Q}$, or more generally,

$$\Re(\text{Tr}(\mathbf{A}\mathbf{B})) = \Re(\text{Tr}(\mathbf{B}\mathbf{A})), \quad \forall \mathbf{A} \in \mathbb{Q}^{d_1 \times d_2}, \mathbf{B} \in \mathbb{Q}^{d_2 \times d_1}. \quad (2.1)$$

We further introduce two key techniques to study quaternion matrices. The first one is the complex or real representation of quaternion matrices based on the maps $\mathcal{T}_{\mathbb{C}}(\cdot)$, $\mathcal{T}(\cdot)$. Note that any $\mathbf{A} \in \mathbb{Q}^{d_1 \times d_2}$ can be uniquely written as $\mathbf{A} = \mathbf{B} + \mathbf{C}\mathbf{j}$ for some $\mathbf{B}, \mathbf{C} \in \mathbb{C}^{d_1 \times d_1}$, then $\mathcal{T}_{\mathbb{C}}(\cdot)$ maps \mathbf{A} to its complex adjoint matrix belonging to $\mathbb{C}^{2d_1 \times 2d_2}$

$$\mathcal{T}_{\mathbb{C}}(\mathbf{A}) := \begin{bmatrix} \mathbf{B} & \mathbf{C} \\ -\mathbf{C} & \mathbf{B} \end{bmatrix}.$$

For quaternion matrices $\mathbf{A}, \mathbf{A}_1, \mathbf{A}_2$, several useful relations are in order:

$$\mathcal{T}_{\mathbb{C}}(\mathbf{A}_1\mathbf{A}_2) = \mathcal{T}_{\mathbb{C}}(\mathbf{A}_1)\mathcal{T}_{\mathbb{C}}(\mathbf{A}_2); \quad \mathcal{T}_{\mathbb{C}}(\mathbf{A}_1 + \mathbf{A}_2) = \mathcal{T}_{\mathbb{C}}(\mathbf{A}_1) + \mathcal{T}_{\mathbb{C}}(\mathbf{A}_2); \quad \mathcal{T}_{\mathbb{C}}(\mathbf{A}^*) = (\mathcal{T}_{\mathbb{C}}(\mathbf{A}))^*; \quad (2.2)$$

see Theorem 4.2 of [68]. Furthermore, $\mathbf{A} \in \mathbb{C}^{d_1 \times d_2}$ can be written as $\mathbf{A} = \mathbf{B} + \mathbf{C}\mathbf{i}$ for some $\mathbf{B}, \mathbf{C} \in \mathbb{R}^{d_1 \times d_2}$, which can then be reduced to real matrix by $\mathcal{T}_{\mathbb{R}}$:

$$\mathcal{T}_{\mathbb{R}}(\mathbf{A}) := \begin{bmatrix} \mathbf{B} & \mathbf{C} \\ -\mathbf{C} & \mathbf{B} \end{bmatrix},$$

and for complex matrices $\mathbf{A}, \mathbf{A}_1, \mathbf{A}_2$ one also has

$$\mathcal{T}_{\mathbb{R}}(\mathbf{A}_1\mathbf{A}_2) = \mathcal{T}_{\mathbb{R}}(\mathbf{A}_1)\mathcal{T}_{\mathbb{R}}(\mathbf{A}_2); \quad \mathcal{T}_{\mathbb{R}}(\mathbf{A}_1 + \mathbf{A}_2) = \mathcal{T}_{\mathbb{R}}(\mathbf{A}_1) + \mathcal{T}_{\mathbb{R}}(\mathbf{A}_2); \quad \mathcal{T}_{\mathbb{R}}(\mathbf{A}^*) = (\mathcal{T}_{\mathbb{R}}(\mathbf{A}))^{\top}. \quad (2.3)$$

Naturally, a composition of these two maps, i.e., $\mathcal{T} := \mathcal{T}_{\mathbb{R}} \circ \mathcal{T}_{\mathbb{C}}$, can reduce $\mathbf{A} \in \mathbb{Q}^{d_1 \times d_2}$ to $\mathcal{T}(\mathbf{A}) \in \mathbb{R}^{4d_1 \times 4d_2}$. More precisely,

$$\mathcal{T}(\mathbf{A}) = \begin{bmatrix} \Re(\mathbf{A}) & \mathcal{P}^{\mathbf{j}}(\mathbf{A}) & \mathcal{P}^{\mathbf{i}}(\mathbf{A}) & \mathcal{P}^{\mathbf{k}}(\mathbf{A}) \\ -\mathcal{P}^{\mathbf{j}}(\mathbf{A}) & \Re(\mathbf{A}) & \mathcal{P}^{\mathbf{k}}(\mathbf{A}) & -\mathcal{P}^{\mathbf{i}}(\mathbf{A}) \\ -\mathcal{P}^{\mathbf{i}}(\mathbf{A}) & -\mathcal{P}^{\mathbf{k}}(\mathbf{A}) & \Re(\mathbf{A}) & \mathcal{P}^{\mathbf{j}}(\mathbf{A}) \\ -\mathcal{P}^{\mathbf{k}}(\mathbf{A}) & \mathcal{P}^{\mathbf{i}}(\mathbf{A}) & -\mathcal{P}^{\mathbf{j}}(\mathbf{A}) & \Re(\mathbf{A}) \end{bmatrix}.$$

A combination of (2.2), (2.3) leads to

$$\mathcal{T}(\mathbf{A}_1\mathbf{A}_2) = \mathcal{T}(\mathbf{A}_1)\mathcal{T}(\mathbf{A}_2); \quad \mathcal{T}(\mathbf{A}_1 + \mathbf{A}_2) = \mathcal{T}(\mathbf{A}_1) + \mathcal{T}(\mathbf{A}_2); \quad \mathcal{T}(\mathbf{A}^*) = (\mathcal{T}(\mathbf{A}))^\top. \quad (2.4)$$

We would also define $\mathcal{T}_i(\mathbf{A})$ ($i = 1, 2, 3, 4$) to be the i -th column of blocks in $\mathcal{T}(\mathbf{A})$. For instance, $\mathcal{T}_1(\mathbf{A}) := [\Re(\mathbf{A})^\top, -\mathcal{P}^j(\mathbf{A})^\top, -\mathcal{P}^i(\mathbf{A})^\top, -\mathcal{P}^k(\mathbf{A})^\top]^\top \in \mathbb{R}^{4d_1 \times d_2}$. From (2.4), $\mathcal{T}_i(\mathbf{A}_1\mathbf{A}_2) = \mathcal{T}(\mathbf{A}_1)\mathcal{T}_i(\mathbf{A}_2)$ follows.

In addition, quaternion singular value decomposition (QSVD) is another powerful tool. For $\mathbf{A} \in \mathbb{Q}^{d_1 \times d_2}$, there exist unitary matrices $\mathbf{U} \in \mathbb{Q}^{d_1 \times d_1}$, $\mathbf{V} \in \mathbb{Q}^{d_2 \times d_2}$, diagonal matrix $\Sigma \in \mathbb{R}^{d_1 \times d_2}$ with non-negative diagonal entries $\sigma_1, \dots, \sigma_{\min\{d_1, d_2\}}$, such that $\mathbf{A} = \mathbf{U}\Sigma\mathbf{V}^*$. We refer readers to Theorem 7.2 in [68] for its derivation. In QSVD, $\{\sigma_k : 1 \leq k \leq \min\{d_1, d_2\}\}$ are the singular values of \mathbf{A} . It is straightforward to show several facts coincident with $\mathbb{R}^{d_1 \times d_2}$ or $\mathbb{C}^{d_1 \times d_2}$, e.g., the maximum singular value equals $\|\mathbf{A}\|$, and $\|\mathbf{A}\|_F = (\sum_k \sigma_k^2)^{1/2}$. Moreover, combining QSVD and the map $\mathcal{T}(\cdot)$ with property (2.4), the SVD for $\mathcal{T}(\mathbf{A})$ is given by $\mathcal{T}(\mathbf{A}) = \mathcal{T}(\mathbf{U})\mathcal{T}(\Sigma)\mathcal{T}(\mathbf{V})^\top$, which leads to $\|\mathcal{T}(\mathbf{A})\| = \|\mathbf{A}\|$, $\|\mathcal{T}(\mathbf{A})\|_F = 2\|\mathbf{A}\|_F$. We will also work with the matrix nuclear norm defined to be the sum of singular values, i.e., $\|\mathbf{A}\|_{nu} = \sum_k \sigma_k$.

For simplicity, in this paper we restrict the eigenvalue to be the right one (But in a complete theory, left eigenvalue and right eigenvalue should be distinguished [68]). In particular, given $\mathbf{A} \in \mathbb{Q}^{d \times d}$, if $\mathbf{A}\mathbf{x} = \mathbf{x}\lambda$ for some nonzero $\mathbf{x} \in \mathbb{Q}^d$, we refer \mathbf{x} , λ to be the eigenvector, eigenvalue of \mathbf{A} . Since $\mathbf{A}\mathbf{x} = \mathbf{x}\lambda$ is equal to $\mathbf{A}(\mathbf{x}v^*) = (\mathbf{x}v^*)(v\lambda v^*)$ for any non-zero $v \in \mathbb{Q}$, \mathbf{A} with eigenvalue λ indeed possesses a set of eigenvalues $\{v\lambda v^* : v \neq 0\}$, among which we can pick a unique "standard eigenvalue" in the form of $a + b\mathbf{i}$ ($a \in \mathbb{R}, b \geq 0$), see Lemma 2.1 in [68]. Any $\mathbf{A} \in \mathbb{Q}^{d \times d}$ has exactly d standard eigenvalues, and particularly, all standard eigenvalues of Hermitian \mathbf{A} are real. Akin to the eigenvalue decomposition for complex Hermitian matrices, quaternion Hermitian matrix \mathbf{A} can be decomposed as $\mathbf{A} = \mathbf{U}\Sigma\mathbf{U}^*$ for some unitary \mathbf{U} and diagonal matrix Σ , with standard eigenvalues of \mathbf{A} arranged in the diagonal of Σ (Corollary 6.2 in [68]).

We need to calculate the derivative of real function with quaternion variable. The framework that best meets such optimization need is the HR calculus, see [35] and the more complete theoretical framework in [65–67]. More precisely, given a function $f(\mathbf{q})$ with quaternion variable $\mathbf{q} = \mathbf{q}_a + \mathbf{q}_b\mathbf{i} + \mathbf{q}_c\mathbf{j} + \mathbf{q}_d\mathbf{k} \in \mathbb{Q}^N$, we define

$$\frac{\partial f}{\partial \mathbf{q}} := \frac{1}{4} \left(\frac{\partial f}{\partial \mathbf{q}_a} - \frac{\partial f}{\partial \mathbf{q}_b}\mathbf{i} - \frac{\partial f}{\partial \mathbf{q}_c}\mathbf{j} - \frac{\partial f}{\partial \mathbf{q}_d}\mathbf{k} \right) \in \mathbb{Q}^N. \quad (2.5)$$

Generally, this is called left derivative and is different from the right derivative $\frac{\partial f}{\partial \mathbf{q}} = \frac{1}{4} \left(\frac{\partial f}{\partial \mathbf{q}_a} - \mathbf{i} \frac{\partial f}{\partial \mathbf{q}_b} - \mathbf{j} \frac{\partial f}{\partial \mathbf{q}_c} - \mathbf{k} \frac{\partial f}{\partial \mathbf{q}_d} \right)$. Considering only the derivative of real function f ($f \in \mathbb{R}$) will be involved in this work, we simply adopt the left one (2.5). For $f \in \mathbb{R}$ with quaternion variable q , $(\frac{\partial f}{\partial q})^*$ represents the direction in which f changes in a maximum rate [35, 66]. Some calculation rules in [66] would also be used later.

3 Quaternion Wirtinger Flow

3.1 The Trivial Ambiguity

Given a quaternion signal $\mathbf{x} \in \mathbb{Q}^d$ and a measurement matrix $\mathbf{A} \in \mathbb{Q}^{n \times d}$, in QPR we aim to reconstruct \mathbf{x} from $\{|\alpha_k^* \mathbf{x}|^2 : k \in [n]\}$, where α_k^* is the k -th row of \mathbf{A} . Observe that for any unit

quaternion q (i.e., $|q| = 1$), $|\mathbf{A}(\mathbf{x}q)|^2 = |\mathbf{A}\mathbf{x}|^2$, so one can never distinguish two signals only differentiated by a global right quaternion phase factor¹. However, a global left quaternion phase factor q is not necessarily an ambiguity since q and \mathbf{A} may not be commutative (hence $|\mathbf{A}(q\mathbf{x})|^2 \neq |\mathbf{A}\mathbf{x}|^2$ is possible)².

Throughout this paper we consider the Gaussian measurement ensemble where the entries of \mathbf{A} are i.i.d. drawn from $\mathcal{N}_{\mathbb{Q}} := \frac{1}{2}\mathcal{N}(0, 1) + \frac{1}{2}\mathcal{N}(0, 1)\mathbf{i} + \frac{1}{2}\mathcal{N}(0, 1)\mathbf{j} + \frac{1}{2}\mathcal{N}(0, 1)\mathbf{k}$, denoted by $\mathbf{A} \sim \mathcal{N}_{\mathbb{Q}}^{n \times d}$. Evidently, $\mathbb{E}\boldsymbol{\alpha}_k\boldsymbol{\alpha}_k^* = \mathbf{I}_d$.

Generally speaking, the goal in any signal reconstruction task is to recover/estimate the signal up to trivial ambiguity. Thus, a question of fundamental importance is whether there exists other unavoidable ambiguities in QPR (besides the right phase factor). In the following, by Mendelson's small ball method, we show the global right quaternion phase factor is the only trivial ambiguity by proving a stronger uniform recovery guarantee: all signals in \mathbb{Q}^d can be reconstructed up to right quaternion phase factor from $O(d)$ phaseless measurements.

Theorem 1. *Assume $\mathbf{A} = [\boldsymbol{\alpha}_1, \dots, \boldsymbol{\alpha}_n]^* \sim \mathcal{N}_{\mathbb{Q}}^{n \times d}$. When $n \geq Cd$ for some absolute constant C , with probability at least $1 - \exp(-C_1n)$, all signals \mathbf{x} in \mathbb{Q}^d can be reconstructed from $\{|\boldsymbol{\alpha}_k^*\mathbf{x}|^2 : k \in [n]\}$ up to a global right quaternion phase factor.*

Proof. We only need to show $|\boldsymbol{\alpha}_k^*\mathbf{x}|^2 = |\boldsymbol{\alpha}_k^*\mathbf{y}|^2$ for all $k \in [n]$ leads to $\mathbf{x}\mathbf{x}^* = \mathbf{y}\mathbf{y}^*$, since this can imply $\mathbf{x} = \mathbf{y} \cdot q$ for some unit quaternion q (This can be verified by a simple element-wise analysis). By (2.1), assuming $\mathbf{x}\mathbf{x}^* \neq \mathbf{y}\mathbf{y}^*$, some algebra gives

$$\begin{aligned} |\boldsymbol{\alpha}_k^*\mathbf{x}|^2 - |\boldsymbol{\alpha}_k^*\mathbf{y}|^2 &= \Re\left[\text{Tr}\left(\boldsymbol{\alpha}_k^*(\mathbf{x}\mathbf{x}^* - \mathbf{y}\mathbf{y}^*)\boldsymbol{\alpha}_k\right)\right] \\ &= \|\mathbf{x}\mathbf{x}^* - \mathbf{y}\mathbf{y}^*\|_F \cdot \Re\left\langle \frac{\mathbf{x}\mathbf{x}^* - \mathbf{y}\mathbf{y}^*}{\|\mathbf{x}\mathbf{x}^* - \mathbf{y}\mathbf{y}^*\|_F}, \boldsymbol{\alpha}_k\boldsymbol{\alpha}_k^* \right\rangle. \end{aligned} \quad (3.1)$$

Recall that $\mathcal{H}_{d,r}^{\mathbb{Q}}$ is the set of all $d \times d$ quaternion Hermitian matrices with rank not exceeding r , and we further let $(\mathcal{H}_{d,r}^{\mathbb{Q}})^* = \mathcal{H}_{d,r}^{\mathbb{Q}} \cap \{\mathbf{X} \in \mathbb{Q}^{d \times d} : \|\mathbf{X}\|_F = 1\}$, then a simple observation is

$$\sum_{k=1}^n (|\boldsymbol{\alpha}_k^*\mathbf{x}|^2 - |\boldsymbol{\alpha}_k^*\mathbf{y}|^2)^2 \geq \|\mathbf{x}\mathbf{x}^* - \mathbf{y}\mathbf{y}^*\|_F^2 \inf_{\mathbf{X} \in (\mathcal{H}_{d,2}^{\mathbb{Q}})^*} [\Re\langle \mathbf{X}, \boldsymbol{\alpha}_k\boldsymbol{\alpha}_k^* \rangle]^2. \quad (3.2)$$

This holds trivially when $\mathbf{x}\mathbf{x}^* = \mathbf{y}\mathbf{y}^*$, and follows from (3.1) when $\mathbf{x}\mathbf{x}^* \neq \mathbf{y}\mathbf{y}^*$. We aim to apply small ball method (Lemma 7) to find a positive lower bound for the empirical process $\inf_{\mathbf{X} \in (\mathcal{H}_{d,2}^{\mathbb{Q}})^*} [\Re\langle \mathbf{X}, \boldsymbol{\alpha}_k\boldsymbol{\alpha}_k^* \rangle]^2$. Firstly, for any $u > 0$ Paley-Zygmund inequality (e.g., Lemma 7.16 in [25]) yields

$$\begin{aligned} Q(u) &:= \inf_{\mathbf{X} \in (\mathcal{H}_{d,2}^{\mathbb{Q}})^*} \mathbb{P}(|\Re\langle \mathbf{X}, \boldsymbol{\alpha}_k\boldsymbol{\alpha}_k^* \rangle| \geq u) \\ &= \inf_{\mathbf{X} \in (\mathcal{H}_{d,2}^{\mathbb{Q}})^*} \mathbb{P}(|\Re\langle \mathbf{X}, \boldsymbol{\alpha}_k\boldsymbol{\alpha}_k^* \rangle|^2 \geq u^2) \geq \inf_{\mathbf{X} \in (\mathcal{H}_{d,2}^{\mathbb{Q}})^*} \frac{(\mathbb{E}|\Re\langle \mathbf{X}, \boldsymbol{\alpha}_k\boldsymbol{\alpha}_k^* \rangle|^2 - u^2)^2}{\mathbb{E}|\Re\langle \mathbf{X}, \boldsymbol{\alpha}_k\boldsymbol{\alpha}_k^* \rangle|^4}. \end{aligned}$$

¹For nonzero quaternion q we call $\frac{q}{|q|}$ its phase. Hence, a global quaternion phase factor, here and hereafter, refers to a unit quaternion number.

²However, when a real measurement matrix is used (as in [16]), this becomes a trivial ambiguity due to $q\mathbf{A} = \mathbf{A}q$ when $\mathbf{A} \in \mathbb{R}^{n \times d}$. This is the essential difference between this work and the QPR result in [16].

Fix any $\mathbf{X} \in (\mathcal{H}_{d,2}^{\mathbb{Q}})^*$ and write it as $\mathbf{X} = \sigma_1 \mathbf{w} \mathbf{w}^* + \sigma_2 \mathbf{v} \mathbf{v}^*$, with $\sigma_1^2 + \sigma_2^2 = 1$, $\sigma_1, \sigma_2 \in \mathbb{R}$, $\|\mathbf{w}\| = \|\mathbf{v}\| = 1$, $\mathbf{w}^* \mathbf{v} = 0$, then $\Re \langle \mathbf{X}, \boldsymbol{\alpha}_k \boldsymbol{\alpha}_k^* \rangle = \sigma_1 |\mathbf{w}^* \boldsymbol{\alpha}_k|^2 + \sigma_2 |\mathbf{v}^* \boldsymbol{\alpha}_k|^2$. By rotational invariance of $\boldsymbol{\alpha}_k$ (Lemma 8(a)), $\mathbf{w}^* \boldsymbol{\alpha}_k$ and $\mathbf{v}^* \boldsymbol{\alpha}_k$ are independent copies of $\frac{1}{2} \mathcal{N}(0, 1) + \frac{1}{2} \mathcal{N}(0, 1) \mathbf{i} + \frac{1}{2} \mathcal{N}(0, 1) \mathbf{j} + \frac{1}{2} \mathcal{N}(0, 1) \mathbf{k}$, hence $4|\mathbf{w}^* \boldsymbol{\alpha}_k|^2$ follows the χ^2 distribution with 4 degrees of freedom. Thus,

$$\begin{aligned} \mathbb{E} [\Re \langle \mathbf{X}, \boldsymbol{\alpha}_k \boldsymbol{\alpha}_k^* \rangle]^2 &= (\sigma_1^2 + \sigma_2^2) \mathbb{E} |\mathbf{w}^* \boldsymbol{\alpha}_k|^4 + 2\sigma_1 \sigma_2 \mathbb{E} |\mathbf{w}^* \boldsymbol{\alpha}_k|^2 \mathbb{E} |\mathbf{v}^* \boldsymbol{\alpha}_k|^2 \\ &\geq \frac{1}{16} \{ \mathbb{E} (4|\mathbf{w}^* \boldsymbol{\alpha}_k|^2)^2 - (\mathbb{E} 4|\mathbf{w}^* \boldsymbol{\alpha}_k|^2)^2 \} = \frac{1}{2}. \end{aligned} \quad (3.3)$$

We can similarly upper bound the denominator and have

$$\begin{aligned} \mathbb{E} |\Re \langle \mathbf{X}, \boldsymbol{\alpha}_k \boldsymbol{\alpha}_k^* \rangle|^4 &= \mathbb{E} (\sigma_1 |\mathbf{w}^* \boldsymbol{\alpha}_k|^2 + \sigma_2 |\mathbf{v}^* \boldsymbol{\alpha}_k|^2)^4 \leq \mathbb{E} (|\mathbf{w}^* \boldsymbol{\alpha}_k|^2 + |\mathbf{v}^* \boldsymbol{\alpha}_k|^2)^4 \\ &= \frac{1}{4^4} \mathbb{E} (4|\mathbf{w}^* \boldsymbol{\alpha}_k|^2 + 4|\mathbf{v}^* \boldsymbol{\alpha}_k|^2)^4 = \frac{2^4 \cdot \Gamma(8)}{4^4 \cdot \Gamma(4)} = \frac{105}{2}. \end{aligned} \quad (3.4)$$

Since (3.3), (3.4) hold for all $\mathbf{X} \in (\mathcal{H}_{d,2}^{\mathbb{Q}})^*$, we have

$$Q\left(\frac{1}{2}\right) \geq \frac{1/16}{105/2} := c_0. \quad (3.5)$$

Secondly, we aim to upper bound $R := \mathbb{E} \sup_{\mathbf{X} \in (\mathcal{H}_{d,2}^{\mathbb{Q}})^*} |\frac{1}{n} \sum_{k=1}^n \varepsilon_k \Re \langle \mathbf{X}, \boldsymbol{\alpha}_k \boldsymbol{\alpha}_k^* \rangle|$ with independent Rademacher variable ε_k . Since for any $\mathbf{A}, \mathbf{B} \in \mathbb{Q}^{d_1 \times d_2}$, $|\langle \mathbf{A}, \mathbf{B} \rangle| \leq \|\mathbf{A}\|_{nu} \|\mathbf{B}\| \leq \sqrt{\text{rank}(\mathbf{A})} \|\mathbf{A}\|_F \|\mathbf{B}\|$ (Lemmas 2.1 and 2.2 in [13]),

$$R = \frac{1}{n} \mathbb{E} \sup_{\mathbf{X} \in (\mathcal{H}_{d,2}^{\mathbb{Q}})^*} \left| \Re \langle \mathbf{X}, \sum_{k=1}^n \varepsilon_k \boldsymbol{\alpha}_k \boldsymbol{\alpha}_k^* \rangle \right| \leq \frac{\sqrt{2}}{n} \mathbb{E} \left\| \sum_{k=1}^n \varepsilon_k \boldsymbol{\alpha}_k \boldsymbol{\alpha}_k^* \right\|.$$

We write $\boldsymbol{\alpha}_k = \boldsymbol{\beta}_k + \gamma_k \mathbf{j}$ where $\boldsymbol{\beta}_k, \gamma_k \in \mathbb{C}^{2d \times 1}$, $2\boldsymbol{\beta}, 2\boldsymbol{\gamma}$ have entries i.i.d. drawn from standard complex Gaussian $\mathcal{N}(0, 1) + \mathcal{N}(0, 1) \mathbf{i}$. Then some calculations give

$$\begin{aligned} \frac{\sqrt{2}}{n} \mathbb{E} \left\| \sum_{k=1}^n \varepsilon_k \boldsymbol{\alpha}_k \boldsymbol{\alpha}_k^* \right\| &= \frac{\sqrt{2}}{n} \mathbb{E} \left\| \sum_{k=1}^n \varepsilon_k (\boldsymbol{\beta}_k + \gamma_k \mathbf{j}) (\boldsymbol{\beta}_k^* - \mathbf{j} \gamma_k^*) \right\| \\ &\leq \frac{\sqrt{2}}{n} \mathbb{E} \left\| \sum_{k=1}^n \varepsilon_k (\boldsymbol{\beta}_k \boldsymbol{\beta}_k^* + \gamma_k \gamma_k^*) \right\| + \frac{\sqrt{2}}{n} \mathbb{E} \left\| \sum_{k=1}^n \varepsilon_k (\gamma_k \boldsymbol{\beta}_k^\top - \boldsymbol{\beta}_k \gamma_k^\top) \right\| \\ &\leq \frac{\sqrt{2}}{n} \left(\mathbb{E} \left\| \sum_{k=1}^n \varepsilon_k \boldsymbol{\beta}_k \boldsymbol{\beta}_k^* \right\| + \mathbb{E} \left\| \sum_{k=1}^n \varepsilon_k \gamma_k \gamma_k^* \right\| + 2 \mathbb{E} \left\| \sum_{k=1}^n \varepsilon_k \gamma_k \boldsymbol{\beta}_k^\top \right\| \right) \leq C_1 \sqrt{\frac{d}{n}} \end{aligned} \quad (3.6)$$

holds for some absolute constant C_1 . The last inequality is from the estimate $\mathbb{E} \left\| \sum_{k=1}^n \varepsilon_k \boldsymbol{\eta}_k \boldsymbol{\eta}_k^* \right\| = O(\sqrt{nd})$ for complex Gaussian $\boldsymbol{\eta}_k$ with i.i.d. entries $\mathcal{N}(0, 1) + \mathcal{N}(0, 1) \mathbf{i}$ (e.g., Lemma 2.7 in [30]), specifically we let $\boldsymbol{\eta}_k^* = (\boldsymbol{\beta}_k^*, \boldsymbol{\gamma}_k^\top)$ and then have

$$O(\sqrt{nd}) = \mathbb{E} \left\| \sum_{k=1}^n \varepsilon_k \boldsymbol{\eta}_k \boldsymbol{\eta}_k^* \right\| = \mathbb{E} \left\| \sum_{k=1}^n \varepsilon_k \begin{bmatrix} \boldsymbol{\beta}_k \boldsymbol{\beta}_k^* & \boldsymbol{\beta}_k \boldsymbol{\gamma}_k^\top \\ \boldsymbol{\gamma}_k \boldsymbol{\beta}_k^* & \boldsymbol{\gamma}_k \boldsymbol{\gamma}_k^\top \end{bmatrix} \right\| \geq \mathbb{E} \left\| \sum_{k=1}^n \varepsilon_k \boldsymbol{\gamma}_k \boldsymbol{\beta}_k^\top \right\|.$$

We now apply Lemma 7, specifically using (A.1) with $u = \frac{1}{4}$, $t = \frac{1}{2}c_0\sqrt{n}$, also combining with (3.5), (3.6). Then it yields that, with probability at least $1 - 2\exp(-\frac{1}{2}c_0^2n)$ we have

$$\inf_{\mathbf{x} \in (\mathcal{H}_{d,2}^{\mathbb{Q}})^*} \frac{1}{n} \sum_{k=1}^n |\Re \langle \mathbf{X}, \boldsymbol{\alpha}_k \boldsymbol{\alpha}_k^* \rangle|^2 \geq \frac{1}{16}c_0 - C_1 \sqrt{\frac{d}{n}} - \frac{c_0}{32} \geq \frac{1}{64}c_0,$$

where the last inequality can be guaranteed under the scaling $n \geq Cd$ for some sufficiently large C . Plug this into (3.2), we obtain

$$\sum_{k=1}^n (|\boldsymbol{\alpha}_k^* \mathbf{x}|^2 - |\boldsymbol{\alpha}_k^* \mathbf{y}|^2)^2 \geq c_2 n \|\mathbf{x}\mathbf{x}^* - \mathbf{y}\mathbf{y}^*\|_F^2$$

Thus, if $|\boldsymbol{\alpha}_k^* \mathbf{x}|^2 = |\boldsymbol{\alpha}_k^* \mathbf{y}|^2$ for all $k \in [n]$, then $\mathbf{x}\mathbf{x}^* = \mathbf{y}\mathbf{y}^*$. The proof is complete. \square

Remark 1. *We stress that extra carefulness is needed to deal with the non-commutativity of quaternion. Specifically, it is crucial for us to take the real part in (3.1), which enables us to swap the multiplication order by (2.1). Note that in general $|\boldsymbol{\alpha}^* \mathbf{x}|^2 \neq \langle \mathbf{x}\mathbf{x}^*, \boldsymbol{\alpha}\boldsymbol{\alpha}^* \rangle$. Indeed, while $\mathbf{x}\mathbf{x}^*$ and $\boldsymbol{\alpha}\boldsymbol{\alpha}^*$ are Hermitian, $\langle \mathbf{x}\mathbf{x}^*, \boldsymbol{\alpha}\boldsymbol{\alpha}^* \rangle$ may be even not real, which is in stark contrast to complex matrices. For example, we can consider $\mathbf{x} = [1, \mathbf{i}]^\top$, $\boldsymbol{\alpha} = [1, \mathbf{j}]^\top$ to check this issue.*

Algebraic argument is another possible approach to show $O(d)$ measurements can lead to uniform recovery of $\mathbf{x} \in \mathbb{Q}^d$ (e.g., [18, 64]). This approach can even derive the minimal measurement number with sharp constant, but usually lacks stability guarantee in a noisy setting. By contrast, with a little bit more work, the statistical approach adopted above directly leads to stability results [14].

3.2 The Algorithm

Recall that WF for solving real/complex phase retrieval problem contains spectral initialization and WF update as two steps [9], and we will first present the QWF algorithm in analogy. We will exclusively use \mathbf{x} to denote the underlying quaternion signal and assume $\|\mathbf{x}\| = 1$, and we focus on the noiseless case for succinctness. In this case, the k -th ($k \in [n]$) phaseless measurement can be formulated as $y_k = |\boldsymbol{\alpha}_k^* \mathbf{x}|^2$.

The QWF algorithm is based on minimizing the ℓ_2 loss

$$\min_{\mathbf{z} \in \mathbb{Q}^d} f(\mathbf{z}) := \frac{1}{n} \sum_{k=1}^n (|\boldsymbol{\alpha}_k^* \mathbf{z}|^2 - y_k)^2.$$

We first describe the careful initialization by spectral method. Consider the Hermitian data matrix

$$\mathbf{S}_{in} = \frac{1}{n} \sum_{k=1}^n y_k \boldsymbol{\alpha}_k \boldsymbol{\alpha}_k^* \quad (3.7)$$

and denote its eigenvector regarding the largest standard eigenvalue by $\boldsymbol{\nu}_{in}$ ($\|\boldsymbol{\nu}_{in}\| = 1$). Intuitively, $\boldsymbol{\nu}_{in}$ can well approximate the direction of \mathbf{x} due to $\mathbb{E}\mathbf{S}_{in} = \mathbf{I}_d + \frac{1}{2}\mathbf{x}\mathbf{x}^*$ (by Lemma

8(d)). While $\mathbb{E}y_k = \|\mathbf{x}\|^2$, it is natural to estimate the signal norm $\|\mathbf{x}\|$ as $(\frac{1}{n} \sum_{k=1}^n y_k)^{1/2}$. Taken collectively, we initialize QWF by setting

$$\mathbf{z}_0 = \left(\frac{1}{n} \sum_{k=1}^n y_k \right)^{1/2} \cdot \mathbf{v}_{in}.$$

Then, QWF refines \mathbf{z}_0 by a quaternion kind of gradient descent, but still termed (Q)WF update by convention. To this end, we first need to calculate $\frac{\partial f}{\partial \mathbf{z}}$ under the framework of (generalized) HR calculus [35,66]. Given $f(\mathbf{z})$ with quaternion variable \mathbf{z} , it would be cumbersome to rewrite it as $f(\Re(\mathbf{z}), \mathcal{P}^i(\mathbf{z}), \mathcal{P}^j(\mathbf{z}), \mathcal{P}^k(\mathbf{z}))$ and then follow the definition (2.5). Instead, we apply some rules derived in [66], specifically the product rule $\frac{\partial(fg)}{\partial \mathbf{q}} = f \frac{\partial g}{\partial \mathbf{q}} + \frac{\partial f}{\partial \mathbf{q}} g$ for real function f, g with quaternion variable \mathbf{q} and a basic result $\frac{\partial |\alpha_k^* \mathbf{z}|^2}{\partial \mathbf{z}} = \frac{1}{2} \mathbf{z}^* \alpha_k \alpha_k^*$ (see Corollary 3.1 and Table IV in [66]). Therefore, the quaternion derivative is given by

$$\begin{aligned} \frac{\partial f(\mathbf{z})}{\partial \mathbf{z}} &= \frac{1}{n} \sum_{k=1}^n \frac{\partial}{\partial \mathbf{z}} (|\alpha_k^* \mathbf{z}|^2 \cdot |\alpha_k^* \mathbf{z}|^2 - 2y_k \cdot |\alpha_k^* \mathbf{z}|^2) \\ &= \frac{2}{n} \sum_{k=1}^n (|\alpha_k^* \mathbf{z}|^2 - y_k) \cdot \frac{\partial |\alpha_k^* \mathbf{z}|^2}{\partial \mathbf{z}} = \frac{1}{n} \sum_{k=1}^n (|\alpha_k^* \mathbf{z}|^2 - |\alpha_k^* \mathbf{x}|^2) \mathbf{z}^* \alpha_k \alpha_k^*. \end{aligned}$$

Hence, taking a suitable step size η , the update rule is

$$\mathbf{z}_{t+1} = \mathbf{z}_t - \eta \cdot \nabla f(\mathbf{z}), \quad (3.8)$$

where we let $\nabla f(\mathbf{z}) := (\frac{\partial f(\mathbf{z})}{\partial \mathbf{z}})^*$ to keep notation light.

3.3 Linear Convergence

For $\mathbf{z}, \mathbf{x} \in \mathbb{Q}^d$, due to the trivial ambiguity of right quaternion phase factor, we characterize the distance between \mathbf{z} and \mathbf{x} by $\text{dist}(\mathbf{z}, \mathbf{x}) = \min_{|w|=1} \|\mathbf{z} - \mathbf{x}w\|$. Define the phase of nonzero $w \in \mathbb{Q}$ to be $\text{sign}(w) = \frac{w}{|w|}$, and let $\text{sign}(0) = 1$, some algebra shows the minimum is attained at $w = \text{sign}(\mathbf{x}^* \mathbf{z})$, and hence $\text{dist}(\mathbf{z}, \mathbf{x}) = \|\mathbf{z} - \mathbf{x} \text{sign}(\mathbf{x}^* \mathbf{z})\|$. In our setting, \mathbf{x} is the fixed underlying signal, hence $\text{dist}(\mathbf{z}, \mathbf{x}) = \|\mathbf{z} - \mathbf{x} \cdot \phi(\mathbf{z})\|$ with $\phi(\mathbf{z}) := \text{sign}(\mathbf{x}^* \mathbf{z})$ describes the reconstruction error of \mathbf{z} . Naturally, a small neighborhood of \mathbf{x} should be given as

$$E_\epsilon(\mathbf{x}) = \{\mathbf{z} \in \mathbb{Q}^d : \text{dist}(\mathbf{z}, \mathbf{x}) \leq \epsilon\}.$$

We present our first main result regarding the linear convergence of QWF.

Theorem 2. *Assume the step size η (3.8) satisfies $0 < \eta \leq \frac{c}{d}$ for sufficiently small c . Then under the sample size $n \geq C_1 d \log n$ for some absolute constant C_1 , with probability at least $1 - C_2 n^{-9} - C_3 n \exp(-C_4 d)$, the sequence $\{\mathbf{z}_t\}$ produced by QWF satisfies*

$$\text{dist}^2(\mathbf{z}_{t+1}, \mathbf{x}) \leq \left(1 - \frac{c_1}{d}\right) \text{dist}^2(\mathbf{z}_t, \mathbf{x}) \quad (3.9)$$

for some c_1 .

The proof of Theorem 2 can be divided into several ingredients below, specifically Lemmas 1–4, and then we will arrive at the desired linear convergence in the end of this Section. The theoretical analysis will be provided in a reverse order. We first show that as long as $\mathbf{z}_0 \in E_\epsilon(\mathbf{x})$ for some sufficiently small ϵ , the sequence produced by QWF update (3.8) linearly converges to \mathbf{x} ; Then, we complete the proof by showing $\mathbf{z}_0 \in E_\epsilon(\mathbf{x})$ holds with high probability. To analyze the behaviour of $\{\mathbf{z}_t\}$ in $E_\epsilon(\mathbf{x})$, we define several conditions to characterize the landscape of $f(\mathbf{z})$ when $\mathbf{z} \in E_\epsilon(\mathbf{x})$.

Condition 1. (Regularity Condition) *The regularity condition holds with positive parameters τ, β, ϵ , abbreviated as RC(τ, β, ϵ), if*

$$\Re \langle \nabla f(\mathbf{z}), \mathbf{z} - \mathbf{x} \cdot \phi(\mathbf{z}) \rangle \geq \frac{1}{\tau} \text{dist}^2(\mathbf{z}, \mathbf{x}) + \frac{1}{\beta} \|\nabla f(\mathbf{z})\|^2, \quad \forall \mathbf{z} \in E_\epsilon(\mathbf{x}). \quad (3.10)$$

With sufficiently small step size, linear convergence of $\{\mathbf{z}_t\}$ can be implied by RC(τ, β, ϵ) of $f(\mathbf{z})$, which is quite analogous to a classical result in convex optimization (Theorem 2.1.15 in [43]) but needs proper modification (Lemma 7.10 in [9]). This remains true in quaternion setting without essential technical changes, hence the proof of Lemma 1 is relegated to Appendix A.

Lemma 1. *Under Condition 1, if $\mathbf{z}_0 \in E_\epsilon(\mathbf{x})$ and the step size $0 < \eta \leq \frac{2}{\beta}$, then the sequence $\{\mathbf{z}_t\}$ produced by (3.8) satisfies*

$$\text{dist}^2(\mathbf{z}_{t+1}, \mathbf{x}) \leq \left(1 - \frac{2\eta}{\tau}\right) \text{dist}^2(\mathbf{z}_t, \mathbf{x}). \quad (3.11)$$

Therefore, it suffices to establish the regularity condition, and similar to [9] we divide it into two properties.

Condition 2. (Local Curvature Condition) *The Local Curvature Condition holds with positive parameters τ, β, ϵ , abbreviated as LCC(τ, β, ϵ), if*

$$\Re \langle \nabla f(\mathbf{z}), \mathbf{z} - \mathbf{x} \phi(\mathbf{z}) \rangle \geq \frac{1}{\tau} \text{dist}^2(\mathbf{z}, \mathbf{x}) + \frac{1}{\beta n} \sum_{k=1}^n |\alpha_k^*(\mathbf{z} - \mathbf{x} \phi(\mathbf{z}))|^4, \quad \forall \mathbf{z} \in E_\epsilon(\mathbf{x}). \quad (3.12)$$

Condition 3. (Local Smoothness Condition) *The Local Smoothness Condition holds with positive parameters τ, β, ϵ , abbreviated as LSC(τ, β, ϵ), if*

$$\|\nabla f(\mathbf{z})\|^2 \leq \frac{1}{\tau} \text{dist}^2(\mathbf{z}, \mathbf{x}) + \frac{1}{\beta} \sum_{k=1}^n \frac{1}{n} |\alpha_k^*(\mathbf{z} - \mathbf{x} \phi(\mathbf{z}))|^4, \quad \forall \mathbf{z} \in E_\epsilon(\mathbf{x}). \quad (3.13)$$

3.3.1 Local Curvature Condition

Lemma 2. (Proving LCC) *Assume $\mathbf{x} \in \mathbb{Q}^d$ is a fixed underlying signal. Given $\epsilon \in [0, 1]$ and sufficiently small $\frac{1}{\tau}, \frac{1}{\beta}$, when $n = \Omega(d \log n)$ for sufficiently large hidden constant, with probability at least $1 - 32n^{-9} - C_1 n \exp(-C_2 d)$, LCC(τ, β, ϵ) in Condition 2 is satisfied.*

Proof. We aim to show (3.12) for some τ, β specified later. We define $\mathbf{h}_0 = \overline{\mathbf{z} \phi(\mathbf{z})} - \mathbf{x}$, then $\mathbf{z} \in E_\epsilon(\mathbf{x})$ translates into $\|\mathbf{h}_0\| \leq \epsilon$, also $\phi(\mathbf{z}) = \text{sign}(\mathbf{x}^* \mathbf{z})$ implies $\Im(\mathbf{h}_0^* \mathbf{x}) = 0$. Then we deal

with (3.12) by using $\nabla f(\mathbf{z}) = \frac{1}{n} \sum_{k=1}^n (|\boldsymbol{\alpha}_k^* \mathbf{z}|^2 - |\boldsymbol{\alpha}_k^* \mathbf{x}|^2) \boldsymbol{\alpha}_k \boldsymbol{\alpha}_k^* \mathbf{z}$ and $\mathbf{z} = (\mathbf{h}_0 + \mathbf{x}) \phi(\mathbf{z})$, it gives a sufficient condition for (3.12) as

$$\begin{aligned} & \frac{2}{n} \sum_{k=1}^n [\Re(\mathbf{x}^* \boldsymbol{\alpha}_k \boldsymbol{\alpha}_k^* \mathbf{h}_0)]^2 + \frac{3}{n} \sum_{k=1}^n |\boldsymbol{\alpha}_k^* \mathbf{h}_0|^2 \Re(\mathbf{x}^* \boldsymbol{\alpha}_k \boldsymbol{\alpha}_k^* \mathbf{h}_0) \\ & + \left(1 - \frac{1}{\beta}\right) \frac{1}{n} \sum_{k=1}^n |\boldsymbol{\alpha}_k^* \mathbf{h}_0|^4 \geq \frac{1}{\tau} \|\mathbf{h}_0\|^2, \quad \forall \|\mathbf{h}_0\| \leq \epsilon, \Im(\mathbf{h}_0^* \mathbf{x}) = 0. \end{aligned} \quad (3.14)$$

We only need to consider nonzero \mathbf{h}_0 and we further let $\mathbf{h}_0 = s \cdot \mathbf{h}$ with $s = \|\mathbf{h}_0\| \in [0, \epsilon]$, $\|\mathbf{h}\| = 1$, $\Im(\mathbf{h}^* \mathbf{x}) = 0$. Hence, (3.14) can be implied by

$$\begin{aligned} & \frac{2}{n} \sum_{k=1}^n [\Re(\mathbf{x}^* \boldsymbol{\alpha}_k \boldsymbol{\alpha}_k^* \mathbf{h})]^2 + \frac{3s}{n} \sum_{k=1}^n |\boldsymbol{\alpha}_k^* \mathbf{h}|^2 \Re(\mathbf{x}^* \boldsymbol{\alpha}_k \boldsymbol{\alpha}_k^* \mathbf{h}) \\ & + \left(1 - \frac{1}{\beta}\right) \frac{s^2}{n} \sum_{k=1}^n |\boldsymbol{\alpha}_k^* \mathbf{h}|^4 \geq \frac{1}{\tau}, \quad \forall \|\mathbf{h}\| = 1, s \in [0, \epsilon], \Im(\mathbf{h}^* \mathbf{x}) = 0. \end{aligned} \quad (3.15)$$

We define $t_\beta := \frac{9}{8(1-\frac{1}{\beta})}$, completing the square, (3.15) is equal to for all $\|\mathbf{h}\| = 1$, $s \in [0, \epsilon]$, $\Im(\mathbf{h}^* \mathbf{x}) = 0$,

$$\frac{1}{n} \sum_{k=1}^n \left(\sqrt{2t_\beta} \Re(\mathbf{x}^* \boldsymbol{\alpha}_k \boldsymbol{\alpha}_k^* \mathbf{h}) + \frac{3s}{\sqrt{8t_\beta}} |\boldsymbol{\alpha}_k^* \mathbf{h}|^2 \right)^2 \geq \frac{1}{\tau} + \frac{2(t_\beta - 1)}{n} \sum_{k=1}^n [\Re(\mathbf{x}^* \boldsymbol{\alpha}_k \boldsymbol{\alpha}_k^* \mathbf{h})]^2. \quad (3.16)$$

We introduce the shorthand $Y_k(\mathbf{h}, s) = \left(\sqrt{2t_\beta} \Re(\mathbf{x}^* \boldsymbol{\alpha}_k \boldsymbol{\alpha}_k^* \mathbf{h}) + \frac{3s}{\sqrt{8t_\beta}} |\boldsymbol{\alpha}_k^* \mathbf{h}|^2 \right)^2$, and $\langle Y_k(\mathbf{h}, s) \rangle = \frac{1}{n} \sum_{k=1}^n Y_k(\mathbf{h}, s)$. By Lemma 8(c) we have $\mathbb{E}[\Re(\mathbf{x}^* \boldsymbol{\alpha}_k \boldsymbol{\alpha}_k^* \mathbf{h})]^2 = \frac{1}{4} + \frac{5}{4} [\Re(\mathbf{x}^* \mathbf{h})]^2$, and we need to work out the concentration of $\frac{1}{n} \sum_{k=1}^n [\Re(\mathbf{x}^* \boldsymbol{\alpha}_k \boldsymbol{\alpha}_k^* \mathbf{h})]^2$ around its mean. Note that $\Re(\mathbf{x}^* \boldsymbol{\alpha}_k \boldsymbol{\alpha}_k^* \mathbf{h})$ is just the $(1, 1)$ -th entry of $\mathcal{T}(\mathbf{x}^* \boldsymbol{\alpha}_k \boldsymbol{\alpha}_k^* \mathbf{h}) = \mathcal{T}(\mathbf{x})^\top \mathcal{T}(\boldsymbol{\alpha}_k) \mathcal{T}(\boldsymbol{\alpha}_k)^\top \mathcal{T}(\mathbf{h})$, we have $\Re(\mathbf{x}^* \boldsymbol{\alpha}_k \boldsymbol{\alpha}_k^* \mathbf{h}) = \mathcal{T}_1(\boldsymbol{\alpha}_k)^\top \mathcal{T}(\mathbf{x}) \mathcal{T}(\mathbf{h})^\top \mathcal{T}_1(\boldsymbol{\alpha}_k) = \sum_{i=1}^4 \mathcal{T}_1(\boldsymbol{\alpha}_k)^\top \mathcal{T}_i(\mathbf{x}) \mathcal{T}_i(\mathbf{h})^\top \mathcal{T}_1(\boldsymbol{\alpha}_k)$, and hence

$$[\Re(\mathbf{x}^* \boldsymbol{\alpha}_k \boldsymbol{\alpha}_k^* \mathbf{h})]^2 = \sum_{i=1}^4 \sum_{j=1}^4 \mathcal{T}_i(\mathbf{h})^\top \left[\left(\mathcal{T}_1(\boldsymbol{\alpha}_k)^\top \mathcal{T}_i(\mathbf{x}) \mathcal{T}_1(\boldsymbol{\alpha}_k)^\top \mathcal{T}_j(\mathbf{x}) \right) \cdot \mathcal{T}_1(\boldsymbol{\alpha}_k) \mathcal{T}_1(\boldsymbol{\alpha}_k)^\top \right] \mathcal{T}_j(\mathbf{h}). \quad (3.17)$$

Letting $Z_k(i, j) = \left(\mathcal{T}_1(\boldsymbol{\alpha}_k)^\top \mathcal{T}_i(\mathbf{x}) \mathcal{T}_1(\boldsymbol{\alpha}_k)^\top \mathcal{T}_j(\mathbf{x}) \right) \cdot \mathcal{T}_1(\boldsymbol{\alpha}_k) \mathcal{T}_1(\boldsymbol{\alpha}_k)^\top$, some algebra gives

$$\left| \frac{1}{n} \sum_{k=1}^n [\Re(\mathbf{x}^* \boldsymbol{\alpha}_k \boldsymbol{\alpha}_k^* \mathbf{h})]^2 - \mathbb{E}[\Re(\mathbf{x}^* \boldsymbol{\alpha}_k \boldsymbol{\alpha}_k^* \mathbf{h})]^2 \right| \leq \sum_{i=1}^4 \sum_{j=1}^4 \left\| \frac{1}{n} \sum_{k=1}^n Z_k(i, j) - \mathbb{E} Z_k(i, j) \right\| \quad (3.18)$$

Note that entries of $\mathcal{T}_1(\boldsymbol{\alpha}_k)$ are independent copies of $\frac{1}{2} \mathcal{N}(0, 1)$, by rotational invariance, without changing distribution we can assume $\mathcal{T}_i(\mathbf{x}) = \mathcal{T}_j(\mathbf{x}) = \mathbf{e}_1$ if $i = j$, or $\mathcal{T}_i(\mathbf{x}) = \mathbf{e}_1$, $\mathcal{T}_j(\mathbf{x}) = \mathbf{e}_2$ if $i \neq j$. Hence, we can invoke Lemma 9 and obtain that when $n = \Omega(\delta^{-2} d \log n)$, the right-hand side of (3.18) is bounded by δ with probability at least $1 - 32n^{-9} - 32 \exp(-\Omega(d))$. This gives rise to $\frac{1}{n} \sum_{k=1}^n [\Re(\mathbf{x}^* \boldsymbol{\alpha}_k \boldsymbol{\alpha}_k^* \mathbf{h})]^2 \leq \frac{1}{4} + \frac{5}{4} [\Re(\mathbf{x}^* \mathbf{h})]^2 + \delta$, hence for showing (3.16), with high probability it suffices to show

$$\langle Y_k(\mathbf{h}, s) \rangle \geq \frac{1}{\tau} + 2(t_\beta - 1) \left(\delta + \frac{1}{4} + \frac{5}{4} [\Re(\mathbf{x}^* \mathbf{h})]^2 \right), \quad \forall \|\mathbf{h}\| = 1, \Im(\mathbf{h}^* \mathbf{x}) = 0, s \in [0, \epsilon]. \quad (3.19)$$

Our strategy is to first consider fixed (\mathbf{h}, s) and then apply a covering argument. Note that

$$\begin{aligned}\mu_k(\mathbf{h}, s) &:= \mathbb{E}Y_k(\mathbf{h}, s) = \frac{9s}{2}\Re(\mathbf{h}^*\mathbf{x}) + \frac{27s^2}{16t_\beta} + \frac{t_\beta}{2} + \frac{5t_\beta}{2}[\Re(\mathbf{x}^*\mathbf{h})]^2 \\ &\leq \frac{9}{2} + 3t_\beta + \frac{27}{16t_\beta} \leq C_1,\end{aligned}\tag{3.20}$$

where we use Lemma 8(b)-(d) in the first line. Assuming $s \leq \epsilon \leq 1$, the last inequality follows as long as $t_\beta = \frac{9}{8(1-\frac{1}{\beta})} = O(1)$. We define $X_k(\mathbf{h}, s) = \mu_k(\mathbf{h}, s) - Y_k(\mathbf{h}, s)$, then $\mathbb{E}X_k(\mathbf{h}, s) = 0$, $X_k(\mathbf{h}, s) \leq \mu_k(\mathbf{h}, s) \leq C_1$. Assuming $t_\beta = O(1)$, we further estimate the variance

$$\begin{aligned}\mathbb{E}[X_k(\mathbf{h}, s)^2] &\leq \mathbb{E}[Y_k(\mathbf{h}, s)^2] = \mathbb{E}\left(\sqrt{2t_\beta}\Re(\mathbf{x}^*\boldsymbol{\alpha}_k\boldsymbol{\alpha}_k^*\mathbf{h}) + \frac{3s}{\sqrt{8t_\beta}}|\boldsymbol{\alpha}_k^*\mathbf{h}|^2\right)^4 \\ &\leq 16\left(4t_\beta^2\mathbb{E}[\Re(\mathbf{x}^*\boldsymbol{\alpha}_k\boldsymbol{\alpha}_k^*\mathbf{h})]^4 + \frac{81}{64t_\beta^2}\mathbb{E}|\boldsymbol{\alpha}_k^*\mathbf{h}|^8\right) \leq C_2.\end{aligned}$$

Now we can invoke Lemma 7.13 in [9] (or the original derivation [6]) and obtain

$$\mathbb{P}\left(\mu_k(\mathbf{h}, s) - \langle Y_k(\mathbf{h}, s) \rangle \geq t\right) \leq \exp(-C_3nt^2), \quad \forall t > 0.\tag{3.21}$$

On the other hand, we can use the first line of (3.20), then for fixed \mathbf{h}, s , (3.19) becomes

$$\langle Y_k(\mathbf{h}, s) \rangle - \mu_k(\mathbf{h}, s) \geq \frac{1}{\tau} + (2t_\beta - 2)\delta - \frac{1}{2} - \frac{5}{2}[\Re(\mathbf{x}^*\mathbf{h})]^2 - \frac{9s}{2}\Re(\mathbf{h}^*\mathbf{x}) - \frac{27s^2}{16t_\beta}.\tag{3.22}$$

Setting ϵ (hence $|s|$), δ , and $\frac{1}{\tau}$ to be sufficiently small, $t_\beta = O(1)$, then the right-hand side of (3.22) can be upper bounded by $-\frac{1}{4}$, hence (3.22) is implied by $\mu_k(\mathbf{h}, s) - \langle Y_k(\mathbf{h}, s) \rangle \leq \frac{1}{4}$. So it remains to show $\sup_{\mathbf{h}, s}(\mu_k(\mathbf{h}, s) - \langle Y_k(\mathbf{h}, s) \rangle) \leq \frac{1}{4}$, where the supremum is taken over $s \in [0, \epsilon]$, $\|\mathbf{h}\| = 1$. For fixed \mathbf{h}, s , by (3.21), $\mathbb{P}(\mu_k(\mathbf{h}, s) - \langle Y_k(\mathbf{h}, s) \rangle \geq \frac{1}{8}) \leq \exp(-\frac{C_3}{64}n)$ holds for any $t \geq 0$. We then apply a covering argument, specifically we construct a δ_s -net \mathcal{N}_s of $[0, \epsilon]$, a $\delta_{\mathbf{h}}$ -net $\mathcal{N}_{\mathbf{h}}$ of $\{\mathbf{h} : \|\mathbf{h}\| = 1\}$, then a union bound delivers

$$\mathbb{P}\left(\max_{s \in \mathcal{N}_s} \max_{\mathbf{h} \in \mathcal{N}_{\mathbf{h}}} [\mu_k(\mathbf{h}, s) - \langle Y_k(\mathbf{h}, s) \rangle] \geq \frac{1}{8}\right) \leq |\mathcal{N}_s||\mathcal{N}_{\mathbf{h}}| \exp(-\frac{C_3}{64}n).\tag{3.23}$$

We can assume $\sup_{s \in [0, \epsilon]} \sup_{\|\mathbf{h}\|=1} [\mu_k(\mathbf{h}, s) - \langle Y_k(\mathbf{h}, s) \rangle] = \mu_k(\mathbf{h}_0, s_0) - \langle Y_k(\mathbf{h}_0, s_0) \rangle$ for some $s_0 \in [0, \epsilon]$, $\|\mathbf{h}_0\| = 1$. We can further pick $\mathbf{h}_1 \in \mathcal{N}_{\mathbf{h}}$, $s_1 \in \mathcal{N}_s$ such that $\|\mathbf{h}_1 - \mathbf{h}_0\| \leq \delta_{\mathbf{h}}$, $|s_1 - s_0| \leq \delta_s$. Similar to [9], for some C_4 , $\max_{k \in [n]} \|\boldsymbol{\alpha}_k\| \leq C_4\sqrt{d}$ holds with probability at least $1 - n \exp(-C_5d)$ (One may also see this by a direction application of Theorem 3.1.1, [60]). We proceed on this assumption, and start from

$$\begin{aligned}& \left| [\mu_k(\mathbf{h}_0, s_0) - \langle Y_k(\mathbf{h}_0, s_0) \rangle] - [\mu_k(\mathbf{h}_1, s_1) - \langle Y_k(\mathbf{h}_1, s_1) \rangle] \right| \\ & \leq \left| \mu_k(\mathbf{h}_0, s_0) - \mu_k(\mathbf{h}_1, s_1) \right| + \left| \frac{1}{n} \sum_{k=1}^n (Y_k(\mathbf{h}_0, s_0) - Y_k(\mathbf{h}_1, s_1)) \right| := R_1 + R_2.\end{aligned}\tag{3.24}$$

We use the first line in (3.20), it is direct to show $R_1 \leq C_6(\delta_{\mathbf{h}} + \delta_s)$. For estimate of R_2 , we let $P_k(\mathbf{h}, s) = \sqrt{2t_\beta}\Re(\mathbf{x}^*\boldsymbol{\alpha}_k\boldsymbol{\alpha}_k^*\mathbf{h}) + \frac{3s}{\sqrt{8t_\beta}}|\boldsymbol{\alpha}_k^*\mathbf{h}|^2$, and note that $Y_k(\mathbf{h}, s) = P_k(\mathbf{h}, s)^2$, $P_k(\mathbf{h}, s) \lesssim d$

due to $t_\beta = O(1)$, $\max_k \|\alpha_k\| \leq C_4 \sqrt{d}$. Then

$$\begin{aligned} R_2 &= \left| \frac{1}{n} \sum_{k=1}^n (P_k(\mathbf{h}_0, s_0) - P_k(\mathbf{h}_1, s_1)) \cdot (P_k(\mathbf{h}_0, s_0) + P_k(\mathbf{h}_1, s_1)) \right| \\ &\lesssim \frac{d}{n} \sum_{k=1}^n \left(|\Re(\mathbf{x}^* \alpha_k \alpha_k^* (\mathbf{h}_0 - \mathbf{h}_1))| + |s_0 - s_1| |\alpha_k^* \mathbf{h}_0|^2 + s_1 (|\alpha_k^* \mathbf{h}_0|^2 - |\alpha_k^* \mathbf{h}_1|^2) \right) \\ &\lesssim d^2 (\delta_{\mathbf{h}} + \delta_s). \end{aligned}$$

Thus, we can take $\delta_{\mathbf{h}}, \delta_s = \frac{1}{C_7 d^2}$ with sufficiently large C_7 so that $R_1 + R_2 \leq \frac{1}{8}$ holds. In this case we can assume $|\mathcal{N}_s| \leq \frac{\epsilon}{1/C_7 d^2} \leq C_7 d^2$, $|\mathcal{N}_{\mathbf{h}}| \leq (1 + 2C_7 d^2)^{4d}$. Plug these into (3.23), when $n = \Omega(d \log d)$ for sufficiently large hidden constant, with probability at least $1 - \exp(-\frac{C_3 n}{128})$, $\max_{s \in \mathcal{N}_s} \max_{\mathbf{h} \in \mathcal{N}_{\mathbf{h}}} [\mu_k(\mathbf{h}, s) - \langle Y_k(\mathbf{h}, s) \rangle] \leq \frac{1}{8}$, which together with (3.24) yields

$$\mu_k(\mathbf{h}_0, s_0) - \langle Y_k(\mathbf{h}_0, s_0) \rangle \leq R_1 + R_2 + \max_{s \in \mathcal{N}_s} \max_{\mathbf{h} \in \mathcal{N}_{\mathbf{h}}} [\mu_k(\mathbf{h}, s) - \langle Y_k(\mathbf{h}, s) \rangle] \leq \frac{1}{4}.$$

Recall that the only additional scaling we assume in the proof is $t_\beta = O(1)$, while this can be guaranteed by sufficiently small $\frac{1}{\beta}$. Hence, the proof is concluded. \square

Remark 2. Compared to the proof in complex case (Section VII of [9]), we need new machinery to deal with some technical issues. For instance, the concentration of $\widehat{R} := \frac{1}{n} \sum_{k=1}^n [\Re(\mathbf{x}^* \alpha_k \alpha_k^* \mathbf{h})]^2$ in (3.18). Specifically, [9] used the concentration of the Hessian matrix $\nabla^2 f(\mathbf{x})$ to govern the whole proof, which could yield the concentration of \widehat{R} by a clever observation $\widehat{R} = \frac{1}{4} \widehat{\mathbf{h}}^* \nabla f(\mathbf{x}) \widehat{\mathbf{h}}$ where $\widehat{\mathbf{h}}^* = [\overline{\mathbf{h}}, \mathbf{h}]$ (Corollary 7.5, [9]). However, this becomes infeasible in quaternion setting: Firstly, the Hessian matrix now contains 16 blocks and can be exhausting in calculations (see (33) in [67]); Perhaps more prominently, the relation between \widehat{R} and $\widehat{\mathbf{h}}^* \nabla f(\mathbf{x}) \widehat{\mathbf{h}}$ heavily relies on commutativity and hence is likely to fail due to non-commutativity of quaternion multiplication. Instead, we calculate $[\Re(\mathbf{x}^* \alpha_k \alpha_k^* \mathbf{h})]^2$ via the real representation $\mathcal{T}(\cdot)$ (3.17). Having reduced to the real case, we directly work on the desired concentration ingredient in Lemma 9.

3.3.2 Local Smoothness Condition

Lemma 3. (Proving LSC) Assume $\mathbf{x} \in \mathbb{Q}^d$ is the fixed underlying signal. Given $\epsilon \in [0, 1]$ and $\tau = C_0$, $\beta = C_1/d$ with sufficiently small C_0, C_1 . If $n = \Omega(d \log n)$ with sufficiently large hidden constant, with probability at least $1 - C_2 n^{-9} - C_3 n \exp(-\Omega(d))$, LSC(τ, β, ϵ) in Condition 3 is satisfied.

Proof. Writing $\|\nabla f(\mathbf{z})\| = \sup_{\|\mathbf{u}\|=1} \Re(\mathbf{u}^* \nabla f(\mathbf{z}))$, the desired LSC(τ, β, ϵ) is equivalent to (τ, β will be specified later)

$$|\Re(\mathbf{u}^* \nabla f(\mathbf{z}))|^2 \leq \frac{1}{\tau} \|\mathbf{z} - \mathbf{x} \phi(\mathbf{z})\|^2 + \frac{1}{\beta} \frac{1}{n} \sum_{k=1}^n |\alpha_k^*(\mathbf{z} - \mathbf{x} \phi(\mathbf{z}))|^4, \quad \forall \mathbf{z} \in E_\epsilon(\mathbf{x}), \|\mathbf{u}\| = 1. \quad (3.25)$$

We let $\mathbf{h} := \overline{\mathbf{z} \phi(\mathbf{z})} - \mathbf{x}$, then $\|\mathbf{h}\| \leq \epsilon$, $\Im(\mathbf{h}^* \mathbf{x}) = 0$, and $\mathbf{z} = (\mathbf{h} + \mathbf{x}) \phi(\mathbf{z})$. Substituting \mathbf{z} with \mathbf{h} , the right-hand side of (3.25) becomes $\frac{1}{\tau} \|\mathbf{h}\|^2 + \frac{1}{\beta} \frac{1}{n} \sum_{k=1}^n |\alpha_k^* \mathbf{h}|^4$. We further define

$\mathbf{w} = \overline{\mathbf{u}\phi(\mathbf{z})}$, and plug in $\nabla f(\mathbf{z})$, some algebra gives

$$\begin{aligned} \Re(\mathbf{u}^* \nabla f(\mathbf{z})) &= \frac{1}{n} \sum_{k=1}^n \left(|\alpha_k^* \mathbf{h}|^2 \Re(\mathbf{w}^* \alpha_k \alpha_k^* \mathbf{h}) + |\alpha_k^* \mathbf{h}|^2 \Re(\mathbf{w}^* \alpha_k \alpha_k^* \mathbf{x}) \right. \\ &\quad \left. + 2\Re(\mathbf{h}^* \alpha_k \alpha_k^* \mathbf{x}) \Re(\mathbf{w}^* \alpha_k \alpha_k^* \mathbf{h}) + 2\Re(\mathbf{h}^* \alpha_k \alpha_k^* \mathbf{x}) \Re(\mathbf{w}^* \alpha_k \alpha_k^* \mathbf{x}) \right). \end{aligned}$$

Thus we can further estimate the left-hand side of (3.25)

$$\begin{aligned} |\Re(\mathbf{u}^* \nabla f(\mathbf{z}))|^2 &\leq \frac{1}{n^2} \left| \sum_{k=1}^n \left(|\alpha_k^* \mathbf{h}|^3 |\alpha_k^* \mathbf{w}| + 3|\alpha_k^* \mathbf{h}|^2 |\alpha_k^* \mathbf{x}| |\alpha_k^* \mathbf{w}| + 2|\alpha_k^* \mathbf{h}| |\alpha_k^* \mathbf{x}|^2 |\alpha_k^* \mathbf{w}| \right) \right|^2 \\ &\leq 3 \left(\left[\frac{1}{n} \sum_{k=1}^n |\alpha_k^* \mathbf{h}|^3 |\alpha_k^* \mathbf{w}| \right]^2 + 9 \left[\frac{1}{n} \sum_{k=1}^n |\alpha_k^* \mathbf{h}|^2 |\alpha_k^* \mathbf{x}| |\alpha_k^* \mathbf{w}| \right]^2 + 4 \left[\frac{1}{n} \sum_{k=1}^n |\alpha_k^* \mathbf{h}| |\alpha_k^* \mathbf{x}|^2 |\alpha_k^* \mathbf{w}| \right]^2 \right) \\ &:= 3(I_1 + 9I_2 + 4I_3). \end{aligned}$$

Similar to the proof of Lemma 2, we can assume $\max_{k \in [n]} \|\alpha_k\| \leq C_1 \sqrt{d}$ with probability at least $1 - n \exp(-cd)$. Since $\|\mathbf{h}\| \leq \epsilon \leq 1$, by Cauchy-Schwarz we have

$$\begin{aligned} I_1 &= \left[\frac{1}{n} \sum_{k=1}^n |\alpha_k^* \mathbf{h}|^3 |\alpha_k^* \mathbf{w}| \right]^2 \lesssim d \cdot \left[\sum_{k=1}^n \left(\frac{1}{\sqrt{n}} |\alpha_k^* \mathbf{h}|^2 \right) \cdot \left(\frac{1}{\sqrt{n}} |\alpha_k^* \mathbf{h}| \right) \right]^2 \\ &\leq d \left(\sum_{k=1}^n \frac{1}{n} |\alpha_k^* \mathbf{h}|^4 \right) \left(\sum_{k=1}^n \frac{1}{n} |\alpha_k^* \mathbf{h}|^2 \right) \lesssim d \left(\sum_{k=1}^n \frac{1}{n} |\alpha_k^* \mathbf{h}|^4 \right) \|\frac{1}{n} \mathbf{A}^* \mathbf{A}\| \lesssim d \left(\sum_{k=1}^n \frac{1}{n} |\alpha_k^* \mathbf{h}|^4 \right), \end{aligned} \quad (3.26)$$

where in the last inequality we use $\|\mathbf{A}^* \mathbf{A}\| \leq \|\mathbf{A}\|^2$ and a standard estimate for operator norm of (sub-)Gaussian matrix that holds with probability at least $1 - 2 \exp(-n)$ (e.g., Theorem 4.4.5, [60]). We similarly use Cauchy-Schwarz to deal with I_2 , it yields

$$\begin{aligned} I_2 &= \left[\sum_{k=1}^n \left(\frac{1}{\sqrt{n}} |\alpha_k^* \mathbf{h}|^2 \right) \left(\frac{1}{\sqrt{n}} |\alpha_k^* \mathbf{x}| |\alpha_k^* \mathbf{w}| \right) \right]^2 \leq \left(\frac{1}{n} \sum_{k=1}^n |\alpha_k^* \mathbf{h}|^4 \right) \left(\frac{1}{n} \sum_{k=1}^n |\alpha_k^* \mathbf{x}|^2 |\alpha_k^* \mathbf{w}|^2 \right) \\ &\leq \left(\frac{1}{n} \sum_{k=1}^n |\alpha_k^* \mathbf{h}|^4 \right) \cdot \left\| \frac{1}{n} \sum_{k=1}^n |\alpha_k^* \mathbf{x}|^2 \alpha_k \alpha_k^* \right\| \lesssim \frac{1}{n} \sum_{k=1}^n |\alpha_k^* \mathbf{h}|^4. \end{aligned}$$

Note that in the last inequality, we can assume $\mathbf{x} = \mathbf{e}_1$ by rotational invariance, then write $\alpha_k = [\alpha_{ki}]$ and calculate

$$\begin{aligned} \left\| \frac{1}{n} \sum_{k=1}^n |\alpha_{k1}|^2 \alpha_k \alpha_k^* \right\| &= \left\| \frac{1}{n} \sum_{k=1}^n |\alpha_{k1}|^2 \mathcal{T}(\alpha_k \alpha_k^*) \right\| \leq \sum_{i=1}^4 \left\| \frac{1}{n} \sum_{k=1}^n |\alpha_{k1}|^2 \mathcal{T}_i(\alpha_k) \mathcal{T}_i(\alpha_k)^\top \right\| \\ &\leq \sum_{i=1}^4 \left\| \frac{1}{n} \sum_{k=1}^n |\Re(\alpha_{k1})|^2 \mathcal{T}_i(\alpha_k) \mathcal{T}_i(\alpha_k)^\top \right\| + \sum_{i=1}^4 \sum_{\vartheta=\mathbf{i}, \mathbf{j}, \mathbf{k}} \left\| \frac{1}{n} \sum_{k=1}^n |\mathcal{P}^\vartheta(\alpha_{k1})|^2 \mathcal{T}_i(\alpha_k) \mathcal{T}_i(\alpha_k)^\top \right\|. \end{aligned} \quad (3.27)$$

Note that $\Re(\alpha_{k1}), \mathcal{P}^\vartheta(\alpha_{k1})$ is just one entry of $\mathcal{T}_i(\alpha_k)$, we can invoke Lemma 9 to establish the concentration of each summand in (3.27) around its mean with $\delta = 1$, while evidently for the

mean of each summand is $O(1)$. This leads to $\left\| \frac{1}{n} \sum_{k=1}^n |\alpha_k^* \mathbf{x}|^2 \alpha_k \alpha_k^* \right\| = O(1)$ with probability at least $1 - C_2 n^{-9} - C_3 \exp(-\Omega(d))$. We use this again to deal with I_3

$$\begin{aligned} I_3 &= \left[\sum_{k=1}^n \left(\frac{1}{\sqrt{n}} |\alpha_k^* \mathbf{h}| |\alpha_k^* \mathbf{x}| \right) \cdot \left(\frac{1}{\sqrt{n}} |\alpha_k^* \mathbf{w}| |\alpha_k^* \mathbf{x}| \right) \right]^2 \\ &\leq \left(\frac{1}{n} \sum_{k=1}^n |\alpha_k^* \mathbf{x}|^2 |\alpha_k^* \mathbf{h}|^2 \right) \cdot \left(\frac{1}{n} \sum_{k=1}^n |\alpha_k^* \mathbf{x}|^2 |\alpha_k^* \mathbf{w}|^2 \right) \lesssim \|\mathbf{h}\|^2. \end{aligned}$$

Putting pieces together, we have shown that for all $\|\mathbf{w}\| = 1$, $\|\mathbf{h}\| \leq \epsilon$, $|\Re(\mathbf{u}^* \nabla f(\mathbf{z}))|^2 \leq C \|\mathbf{h}\|^2 + Cd \left(\frac{1}{n} \sum_{k=1}^n |\alpha_k^* \mathbf{h}|^4 \right)$. Thus, $\text{LSC}(\tau, \beta, \epsilon)$ holds with sufficiently small τ , and $\beta = \frac{c_1}{d}$ with sufficiently small c_1 . The result follows. \square

3.3.3 Spectral Initialization

Now it is clear that, for some sufficiently small $\frac{1}{\beta_1}, \beta_2$, $\text{LCC}(\beta_1, \beta_1, \epsilon)$ and $\text{LSC}(\beta_2, \beta_2/d, \epsilon)$ hold simultaneously, which directly leads to $\text{RSC}(2\beta_1 d, \frac{\beta_1}{\beta_2} d, \epsilon)$. By Lemma 1, the QWF sequence with $\eta \leq \frac{2}{d}$ linearly converges to \mathbf{x} if some iteration point is sufficiently close to \mathbf{x} . Thus, the proof can be concluded by showing $\mathbf{z}_0 \in E_\epsilon(\mathbf{x})$, which is presented in Lemma 4. The proof is parallel to the complex case, so we provide it in Appendix.

Lemma 4. *Assume \mathbf{x} is the fixed underlying signal. Given $\delta \in (0, 1]$. If $n \geq C_0 \delta^{-2} d \log n$ for sufficiently large hidden constant, then with probability at least $1 - C_1 n^{-9} - C_2 \exp(-C_3 d)$, $\mathbf{z}_0 \in E_{2\delta}(\mathbf{x})$.*

In Lemma 4 we take $\delta = \frac{1}{16}$, then under the assumptions of Theorem 2 $\mathbf{z}_0 \in E_{1/8}(\mathbf{x})$ with high probability. Then, applying Lemma 2, 3 shows $\text{RSC}(c, dc, \frac{1}{8})$ (where c is sufficiently large). Thus, if $\eta = O(\frac{1}{d})$, Lemma 1 delivers the linear convergence claimed in Theorem 2.

Remark 3. (Refine the step size) *The step size can be enlarged to $O(1)$ when $\mathbf{z}_t \in E_{O(1/n)}(\mathbf{x})$ because the estimate (3.26) can be tightened to $\frac{1}{n} \sum_{k=1}^n |\alpha_k^* \mathbf{h}|^4$, which delivers $\text{LSC}(\tau, \beta, \epsilon)$ with $\tau, \beta = O(1)$. This also explains the adaptive step size in [9].*

Remark 4. (Stability of QWF) *One can also explore the stability of QWF in a noisy setting. We refer interesting readers to Theorem 12.3.2 in [53] but do not pursue this here.*

3.4 Variants of Quaternion Wirtinger Flow

While WF may be the most popular non-convex optimization approach for phase retrieval, there exist many variants that refine WF from different respects, and representatives include truncated Wirtinger flow (TWF) [15], truncated amplitude flow (TAF) [62]. For example, by a truncation technique, in TWF both spectral initialization and WF update are conducted in a more selective manner. Accordingly, we also propose the quaternion version of QWF, QAF (naturally abbreviated as QTWF, QTAF) in Appendix B. We numerically test their performance without pursuing a theoretical proof³. It turns out that their experimental improvements are still quite notable in QPR (e.g., the performance under insufficient measurements, larger step size), as we shall see their experimental results in Section 5.

³Taking the set of techniques used in this work, a proof would be possible, but also extremely tedious. Note that even in [15] (TWF) and [62] (TAF), the proofs are only provided for the real case (i.e., real \mathbf{A}, \mathbf{x}), while the complex case is only numerically simulated.

4 Pure Quaternion Wirtinger Flow

A quaternion number is said to be pure quaternion if it has zero real part. We define the set of pure quaternion to be $\mathbb{Q}_p = \{q \in \mathbb{Q} : \Re(q) = 0\}$, and \mathbb{Q}_p^d represents the space of d -dimensional pure quaternion vectors/signals. This section is intended to propose a variant of QWF called pure quaternion Wirtinger flow (PQWF) that can effectively utilize the priori of $\mathbf{x} \in \mathbb{Q}_p^d$. This is motivated, for example, by quaternion methods in color image processing where the color channels are encoded in three imaginary components, and hence the desired signal is pure quaternion [17, 31]. While many works choose to remove the real part of the quaternion signal after the reconstruction (e.g., [17, 31, 40]), it is obviously more sensible to incorporate the pure quaternion priori into the recovery procedure and gain some benefits [13, 54].

For $\mathbf{a} \in \mathbb{Q}^d$ we define the real counterpart $\mathcal{V}(\mathbf{a}) := [\Re(\mathbf{a}), \mathcal{P}^i(\mathbf{a}), \mathcal{P}^j(\mathbf{a}), \mathcal{P}^k(\mathbf{a})] \in \mathbb{R}^{d \times 4}$. For instance, we have $\mathcal{V}(\mathbf{x}) = [\mathbf{0}, \mathcal{P}^i(\mathbf{x}), \mathcal{P}^j(\mathbf{x}), \mathcal{P}^k(\mathbf{x})]$ if $\mathbf{x} \in \mathbb{Q}_p^d$. In what follows we show that, for pure quaternion signal \mathbf{x} satisfying $\text{rank}(\mathcal{V}(\mathbf{x})) = 3$, or in other words, three imaginary components of \mathbf{x} are real linearly independent, the trivial ambiguity in QPR reduces to a sign.

Lemma 5. *Assume $\mathbf{x} \in \mathbb{Q}_p^d$. In the phase-less measurement setting described in Theorem 1, all \mathbf{x} satisfying $\text{rank}(\mathcal{V}(\mathbf{x})) = 3$ can be reconstructed from $\{|\boldsymbol{\alpha}_k^* \mathbf{x}|^2 : k \in [n]\}$ up to a sign ± 1 .*

Proof. By Theorem 1, one can exactly reconstruct $\mathcal{A}_x := \{\mathbf{x}q : q \in \mathbb{Q}, |q| = 1\}$. Due to the assumption of $\mathbf{x} \in \mathbb{Q}_p^d$, we choose $\mathbf{x}_0 \in \mathcal{A}_x$ and further pick $q = q_0 + q_1 \mathbf{i} + q_2 \mathbf{j} + q_3 \mathbf{k}$ with $|q| = 1$ such that $\Re(\mathbf{x}_0 q) = (\Re \mathbf{x}_0)q_0 - (\mathcal{P}_i \mathbf{x}_0)q_1 - (\mathcal{P}_j \mathbf{x}_0)q_2 - (\mathcal{P}_k \mathbf{x}_0)q_3 = 0$. It is not hard to verify that $\text{rank}(\mathcal{V}(\mathbf{x}_0)) = \text{rank}(\mathcal{V}(\mathbf{x})) = 3$, for example, one can identify $\mathcal{V}(\mathbf{x}_0)$ with the first row of $\mathcal{T}(\mathbf{x}_0)$ up to permutation and then use $\mathcal{T}(\mathbf{x}_0 q) = \mathcal{T}(\mathbf{x}_0)\mathcal{T}(q)$. Thus, $[q_0, q_1, q_2, q_3]^\top$ lives in a one-dimensional subspace of \mathbb{R}^4 . Combining with $|q| = 1$, there are only two feasible q in the form of $\{\hat{q}, -\hat{q}\}$, and $\pm \mathbf{x}_0 \hat{q}$ obviously corresponds to $\pm \mathbf{x}$. \square

Remark 5. *We remark that for color images with red, green, blue channels, each pixel has non-negative imaginary parts in its pure quaternion representation. Thus, the ambiguity of the sign (± 1) can be further removed, meaning that the image can be exactly reconstructed.*

Since $\text{rank}(\mathcal{V}(\mathbf{x})) = 3$ is extremely minor for application, we impose this assumption and define $\text{dist}_p(\mathbf{z}, \mathbf{x}) = \min\{\|\mathbf{z} + \mathbf{x}\|, \|\mathbf{z} - \mathbf{x}\|\}$ to measure the reconstruction error. Note that the convergence guarantee for QWF is under the error metric $\text{dist}(\mathbf{z}_t, \mathbf{x}) = \|\mathbf{z}_t - \mathbf{x}\phi(\mathbf{z}_t)\|$, or equivalently, $\{\mathbf{z}_t \phi(\mathbf{z}_t)\}$ linearly converges to \mathbf{x} , but the issue is that $\phi(\mathbf{z}_t) = \text{sign}(\mathbf{z}_t^* \mathbf{x})$ can never be determined. Thus, additional efforts are needed to design an algorithm for phase retrieval of $\mathbf{x} \in \mathbb{Q}_p^d$ with convergence guarantee regarding $\text{dist}_p(\mathbf{z}_t, \mathbf{x})$.

While $\phi(\mathbf{z}_t)$ is in general unknown, our idea here is to estimate it up to a sign based on the pure quaternion priori. More precisely, we find a unit quaternion q_t such that $\mathbf{z}_t q_t$ is closest to pure quaternion signal, i.e.,

$$q_t = \arg \min_{|q|=1} \|\Re(\mathbf{z}_t q)\|. \quad (4.1)$$

A simple observation is $\|\Re(\mathbf{z}_t q)\| = \|\mathcal{V}(\mathbf{z}_t)\mathcal{V}^\top(\bar{q})\|$, thus (4.1) is equal to finding the eigenvector with respect to the smallest eigenvalue of $\mathcal{V}(\mathbf{z}_t)^\top \mathcal{V}(\mathbf{z}_t) \in \mathbb{R}^{4 \times 4}$, which can be implemented efficiently and cheaply without inducing a higher computational complexity of QWF.

The following condition on \mathbf{x} assumes a scaling slightly stronger than $\text{rank}(\mathcal{V}(\mathbf{x})) = 3$, i.e., the third singular value of $\mathcal{V}(\mathbf{x})$ is bounded away from 0. We restrict our analysis to the set of pure quaternion signals with Condition 4 for some absolute constant κ_0 .

Condition 4. The pure quaternion signal \mathbf{x} has unit ℓ_2 norm, and $\mathcal{V}(\mathbf{x})$ has three positive singular values bounded below by (i.e., larger than) some absolute constant κ_0 ($\kappa_0 > 0$).

The following Lemma shows q_t found by (4.1) can transfer the error metric from $\text{dist}(\mathbf{z}_t, \mathbf{x})$ to $\text{dist}_p(\mathbf{z}_t q_t, \mathbf{x})$, with the error preserved up to a multiplicative constant only related to κ_0 in Condition 4.

Lemma 6. Under Condition 4 we assume $\text{dist}(\mathbf{z}_t, \mathbf{x}) \leq \delta$ for $\delta \in (0, \frac{1}{2})$. If the quaternion phase factor q_t is found by (4.1), it holds that $\text{dist}_p(\mathbf{z}_t q_t, \mathbf{x}) \leq (\frac{6}{\kappa_0} + 1) \text{dist}(\mathbf{z}_t, \mathbf{x})$.

Proof. We let $\hat{\mathbf{z}}_t = \mathbf{z}_t \overline{\phi(\mathbf{z}_t)}$, then $\text{dist}(\mathbf{z}_t, \mathbf{x}) = \|\hat{\mathbf{z}}_t - \mathbf{x}\| = \|\mathcal{V}(\hat{\mathbf{z}}_t) - \mathcal{V}(\mathbf{x})\|_F$. Hence, $\|\hat{\mathbf{z}}_t\| \leq \|\hat{\mathbf{z}}_t - \mathbf{x}\| + \|\mathbf{x}\| \leq 1 + \delta \leq \frac{3}{2}$. Evidently, $w_t = \phi(\mathbf{z}_t) q_t$ is the solution of $\min_{|w|=1} \|\Re(\hat{\mathbf{z}}_t w)\|$. Note that $|w_t| = 1$, we have

$$\begin{aligned} \text{dist}_p(\mathbf{z}_t q_t, \mathbf{x}) &= \text{dist}_p(\hat{\mathbf{z}}_t w_t, \mathbf{x}) = \min\{\|\hat{\mathbf{z}}_t w_t - \mathbf{x}\|, \|\hat{\mathbf{z}}_t w_t + \mathbf{x}\|\} \\ &\leq \min\{\|\hat{\mathbf{z}}_t w_t - \hat{\mathbf{z}}_t\|, \|\hat{\mathbf{z}}_t w_t + \hat{\mathbf{z}}_t\|\} + \|\hat{\mathbf{z}}_t - \mathbf{x}\| \leq \frac{3}{2} \min\{|w_t - 1|, |w_t + 1|\} + \text{dist}(\mathbf{z}_t, \mathbf{x}) \\ &\leq \frac{3}{2} |\Im(w_t)| + \frac{3}{2} \min\{1 - \Re(w_t), 1 + \Re(w_t)\} + \text{dist}(\mathbf{z}_t, \mathbf{x}) \\ &\leq \frac{3}{2} |\Im(w_t)| + \frac{3}{2} |\Im(w_t)|^2 + \text{dist}(\mathbf{z}_t, \mathbf{x}) \leq 3 |\Im(w_t)| + \text{dist}(\mathbf{z}_t, \mathbf{x}). \end{aligned} \tag{4.2}$$

Moreover, we have

$$\begin{aligned} \|\Re(\mathbf{x} w_t)\| &\leq \|\Re((\mathbf{x} - \hat{\mathbf{z}}_t) w_t)\| + \|\Re(\hat{\mathbf{z}}_t w_t)\| \leq \text{dist}(\mathbf{z}_t, \mathbf{x}) + \|\Re(\hat{\mathbf{z}}_t)\| \\ &\leq \text{dist}(\mathbf{z}_t, \mathbf{x}) + \|\Re(\hat{\mathbf{z}}_t - \mathbf{x})\| \leq 2 \text{dist}(\mathbf{z}_t, \mathbf{x}), \end{aligned}$$

where we use the optimality of w_t in the second inequality. On the other hand, by Condition 4 $\|\Re(\mathbf{x} w_t)\| = \|\mathcal{V}(\mathbf{x}) \mathcal{V}_1(w_t)\| \geq \kappa_0 |\Im(w_t)|$. Combining these two relations, we obtain $|\Im(w_t)| \leq \frac{2}{\kappa_0} \text{dist}(\mathbf{z}_t, \mathbf{x})$. Substitute this into (4.2), the proof is concluded. \square

Now we are at a position to propose the PQWF algorithm. Compared with QWF, the spectral initialization \mathbf{z}_0 and QWF update in (3.8) remain unchanged, and the only difference is that we pick a positive integer T_p and then map \mathbf{z}_t to $\Im(\mathbf{z}_t q_t)$ every T_p QWF updates. That is to say, for each non-negative integer k we change \mathbf{z}_{kT} to the pure quaternion signal $\tilde{\mathbf{z}}_{kT_p} := \Im(\mathbf{z}_{kT_p} \cdot q_{kT_p})$, then proceed the next QWF update as $\mathbf{z}_{kT_p+1} = \tilde{\mathbf{z}}_{kT_p} - \eta \nabla f(\tilde{\mathbf{z}}_{kT_p})$. Specifically, the initialization now becomes $\tilde{\mathbf{z}}_0 = \Im(\mathbf{z}_0 q_0)$, which still falls into a small neighbourhood of \mathbf{x} (i.e., $E_{\delta,p}(\mathbf{x}) = \{\mathbf{z} \in \mathbb{Q}^d : \text{dist}_p(\mathbf{z}, \mathbf{x}) \leq \delta\}$) with high probability, due to the combination of Lemma 4 and Lemma 6. Thus, with proper T_p , the linear convergence of PQWF can be established.

Theorem 3. We consider \mathbf{x} satisfying Condition 4. Suppose we are in the setting of Theorem 2, with the difference that we map \mathbf{z}_{kT_p} to $\tilde{\mathbf{z}}_{kT_p} := \Im(\mathbf{z}_{kT_p} \cdot q_{kT_p})$ for each non-negative integer k , where q_{kT_p} is defined in (4.1). Assume (3.9) holds for some c_1 , then by Lemma 6

$$\text{dist}_p^2(\tilde{\mathbf{z}}_{kT_p}, \mathbf{x}) \leq \text{dist}_p^2(\mathbf{z}_{kT_p} \cdot q_{kT_p}, \mathbf{x}) \leq c_2 \text{dist}^2(\mathbf{z}_{kT_p}, \mathbf{x})$$

holds for some $c_2 > 1$. Then if $T_p \geq \frac{-2 \log(c_2)}{\log(1 - c_1/d)}$, we have

$$\text{dist}_p^2(\tilde{\mathbf{z}}_{(k+1)T_p}, \mathbf{x}) \leq \left(1 - \frac{c_1}{4d}\right)^{T_p} \text{dist}_p^2(\tilde{\mathbf{z}}_{kT_p}, \mathbf{x}), \quad \forall k \geq 0. \tag{4.3}$$

Proof. Starting from $\tilde{\mathbf{z}}_{kT_p}$, T_p QWF updates give $\mathbf{z}_{(k+1)T_p}$, since (3.9) holds for some c_1 , we have $\text{dist}^2(\mathbf{z}_{(k+1)T_p}, \mathbf{x}) \leq (1 - \frac{c_1}{d})^{T_p} \text{dist}^2(\tilde{\mathbf{z}}_{kT_p}, \mathbf{x})$. Moreover, by assumption $\text{dist}_p^2(\tilde{\mathbf{z}}_{(k+1)T_p}, \mathbf{x}) \leq c_2 \text{dist}^2(\mathbf{z}_{(k+1)T_p}, \mathbf{x})$. Combining them, we obtain

$$\text{dist}_p^2(\tilde{\mathbf{z}}_{(k+1)T_p}, \mathbf{x}) \leq c_2 (1 - \frac{c_1}{d})^{T_p} \text{dist}^2(\tilde{\mathbf{z}}_{kT_p}, \mathbf{x}) \leq (1 - \frac{c_1}{d})^{T_p/2} \text{dist}^2(\tilde{\mathbf{z}}_{kT_p}, \mathbf{x}),$$

where we use $T_p \geq \frac{-2 \log(c_2)}{\log(1 - c_1/d)}$ in the last inequality. Further use $\sqrt{1 - \frac{c_1}{d}} \leq 1 - \frac{c_1}{4d}$ and $\text{dist}(\mathbf{a}, \mathbf{b}) \leq \text{dist}_p(\mathbf{a}, \mathbf{b})$, the result follows. \square

In the next section, we will test the performance of PQWF for the recovery of pure quaternion signal.

5 Experimental Results

We present experimental results in this Section, specifically Section 5.1 for synthetic data, Section 5.2 for color images, and Section 5.3 for two variants of QWF⁴.

5.1 Synthetic Data

In each single trial of QWF, we use Gaussian measurement ensemble $\mathbf{A} \sim \mathcal{N}_{\mathbb{Q}}^{n \times d}$. The entries of quaternion signal $\mathbf{x} \in \mathbb{Q}^d$ (resp. pure quaternion signal $\mathbf{x} \in \mathbb{Q}_p^d$) are i.i.d. copies of $\mathcal{N}(0, 1) + \sum_{\vartheta=i,j,k} \mathcal{N}(0, 1)\vartheta$ (resp. $\sum_{\vartheta=i,j,k} \mathcal{N}(0, 1)\vartheta$), then \mathbf{x} will be normalized so that $\|\mathbf{x}\| = 1$. We apply 100 power iterations to approximately find the \mathbf{v}_{in} as the leading eigenvector of the Hermitian \mathbf{S}_{in} . Here, the power method for quaternion Hermitian matrix is parallel to the complex case [34]. By default, we set $\eta = 0.2$ and run 1500 QWF updates to obtain the reconstructed signal $\hat{\mathbf{z}}$.

We first report the success rate of QWF under different sample sizes (Figure 1(a)). Specifically, we test $d = 100$ and the sample sizes $\frac{n}{d} = 3 : 0.5 : 13$. For each n we conduct 100 independent trials, with a trial claimed to be success if $\text{dist}(\hat{\mathbf{z}}, \mathbf{x}) < 10^{-5}$ [9, 15]. One can see that the phase transition starts from $n/d = 6.5$, and the success rate reaches 1 at $n/d = 9$. Under $n \geq 9d$ the success rate remains to be 1, meaning that such sample size is sufficient for QWF to succeed. In Figure 1(b), we also plot the curve of $\log(\text{dist}(\mathbf{z}_t, \mathbf{x}))$ versus t in a single trial with $m/n = 10$ and 3500 QWF updates. The curve decreases and shapes like a straight line, and then reaches a plateau, which is consistent with our linear convergence guarantee in Theorem 2 (3.9).

Then we go into pure quaternion signal reconstruction via PQWF, and we test $\mathbf{x} \in \mathbb{Q}_p^{50}$. Note that the error metric now becomes $\text{dist}_p(\mathbf{z}, \mathbf{x}) = \min\{\|\mathbf{z} + \mathbf{x}\|, \|\mathbf{z} - \mathbf{x}\|\}$ since the synthetic signal of course admits Condition 4. By comparing several algorithms, our main goal is to show the proposed PQWF in Section 4 can effectively incorporate the pure quaternion priori and gain notable benefits from it, e.g., earlier phase transition. The first competitor (Alg. I) is QWF that does not embed the priori into iteration but only finally maps the obtained $\hat{\mathbf{z}}$ to $\Im(\hat{\mathbf{z}}\hat{q})$ where \hat{q} is the solution to (4.1) with $\mathbf{z}_t = \hat{\mathbf{z}}$. We still have two other competitors (Alg. II, Alg. III) that apply the pure quaternion priori by directly removing the real part

⁴Our implementation is based on the quaternion toolbox for Matlab developed by S. J. Sangwine and N. Le Bihan available in <https://sourceforge.net/projects/qt4m/>.

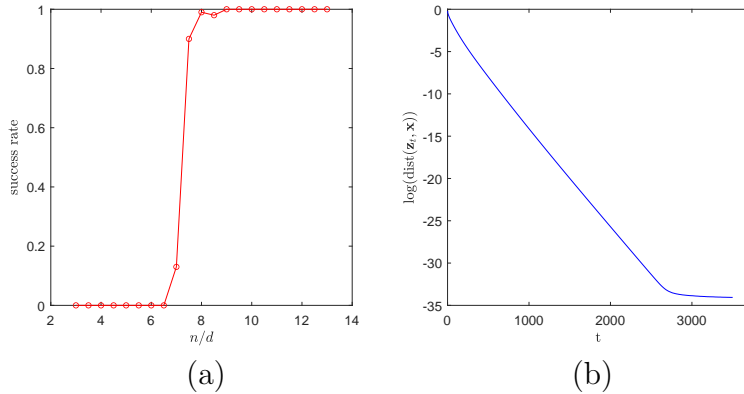


Figure 1: (a): success rate of QWF under different sample sizes; (b): linear convergence.

without estimating the right quaternion phase factor like (4.1). It should be stressed that this is indeed an intuitive way to enforce the pure quaternion constraint, and has been widely adopted in related works. More specifically, Alg. II imposes the pure quaternion constraint every T_p updates, but different from PQWF that maps \mathbf{z}_{kT_p} to $\mathfrak{S}(\mathbf{z}_{kT_p} \cdot q_{kT_p})$, Alg. III maps \mathbf{z}_{kT_p} to $\mathfrak{S}(\mathbf{z}_{kT_p})$ when $k \geq 1$ (i.e., except for the spectral initialization). Akin to Alg. I, Alg. III only employs the priori after the whole procedure of QWF, but it maps the returned signal $\hat{\mathbf{z}}$ to $\mathfrak{S}(\hat{\mathbf{z}})$ (rather than $\mathfrak{S}(\hat{\mathbf{z}} \cdot \hat{q})$). The experimental results are reported in Figure 2.

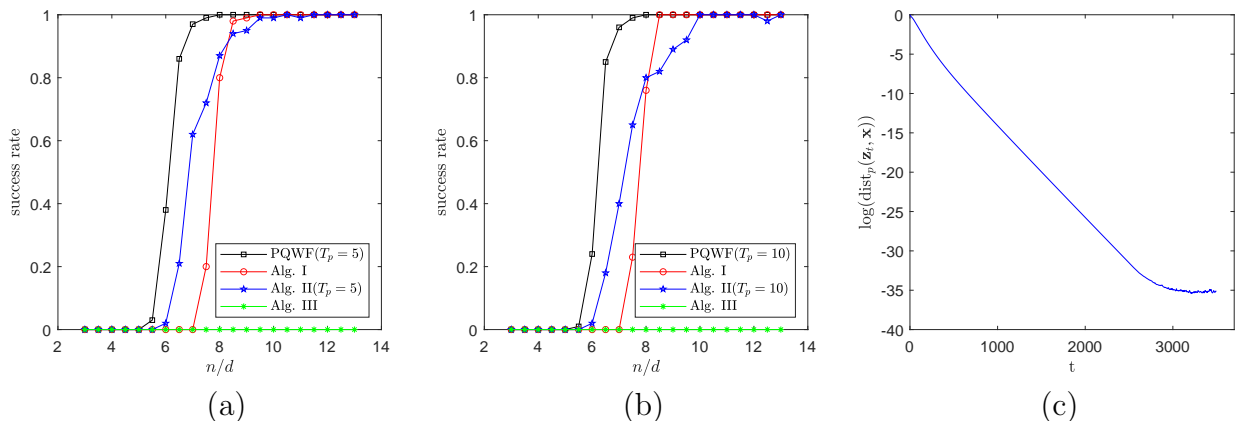


Figure 2: (a) and (b): Success rate of PQWF and Alg. I–III under different sample sizes, with $T_p = 5$ or $T_p = 10$; (c): linear convergence.

We provide the success rate of PQWF and Alg. I–III under $\frac{m}{n} = 3 : 0.5 : 13$ in Figure 2(a) (for $T_p = 5$) and Figure 2(b) (for $T_p = 10$). One shall see that the proposed PQWF outperforms Alg. I–III. For instance, it embraces a phase transition earlier than Alg. I, thus confirming the efficacy of PQWF in utilizing the pure quaternion priori to reduce the measurement number. In stark contrast, imposing the pure quaternion constraint by removing the real part, Alg. II and Alg. III have worse performances, which demonstrates the crucial role played by the phase factor estimate (4.1). Since $\hat{\mathbf{z}}$ returned by QWF only recovers \mathbf{x} up to the unknown right quaternion phase factor, $\mathfrak{S}(\hat{\mathbf{z}})$ obviously does not approximate \mathbf{x} up to a sign. Thus, the complete failure of Alg. III is expected. On the other hand, it would be more interesting to take a closer look at the curve of Alg. II. In particular, Alg. II also enjoys an phase transition earlier than Alg. I ($6 \leq \frac{n}{d} \leq 7$), so removing the real part every T_p updates seems a bit

rational. However, under relatively sufficient measurements (e.g., $8.5 \leq \frac{n}{d} \leq 10$, Figure 2(b)), it can be even worse than Alg. I. For illustration, we comment that the QWF update is based on the data, while removing the real part is based on the priori. Thus, they are indeed totally independent procedures, so their effects on the sequence are likely to somehow neutralize, which possibly explains the unsatisfactory performance of Alg. II.

Beyond that, we also track $\log(\text{dist}_p(\tilde{\mathbf{z}}_{5k}, \mathbf{x}))$ in a single trial of PQWF with $T_p = 5$, $m/n = 8$, and then plot the error decreasing curve in Figure 2(c). This corroborates our linear convergence guarantee (4.3).

5.2 Color Image

In this part, we test our algorithms in real data. Specifically, we implement PQWF in color images to confirm its practicality in phaseless image restoration. The tested 256×256 images "Female" and "Mandrill" are available online⁵. Due to the memory limit, it is not possible to possess the whole color image as a pure quaternion signal with length 256^2 , e.g., even the measurement matrix $\mathbf{A} \in \mathbb{Q}^{n \times 256^2}$ cannot be drawn. Indeed, to handle extremely huge image one needs measurement ensemble that is essentially cheaper in memory and computation, e.g., coded diffraction pattern (CDP) [8], as adopted for imaging experiments in [9, 15, 62]. Unfortunately, CDP for quaternion signal is yet to design, not to mention the theory of QWF under CDP, which is left as future work.

To circumvent this issue, the image is divided into blocks of size 16×16 , which are then represented as the underlying signal $\mathbf{x} \in \mathbb{Q}_p^{256}$. Then, we deal with each block separately, and we can still adopt $\mathbf{A} \in \mathcal{N}_{\mathbb{Q}}^{m \times 256}$ with $m = 9 * 256$ and invoke PQWF for recovery, with 1500 QWF updates ($T_p = 5$) and suitable step size. Recall that a color image can be exactly reconstructed without any ambiguity (Remark 5). We show the original images, reconstructed images in Figure 3, and report that both relative errors are smaller than 10^{-9} .

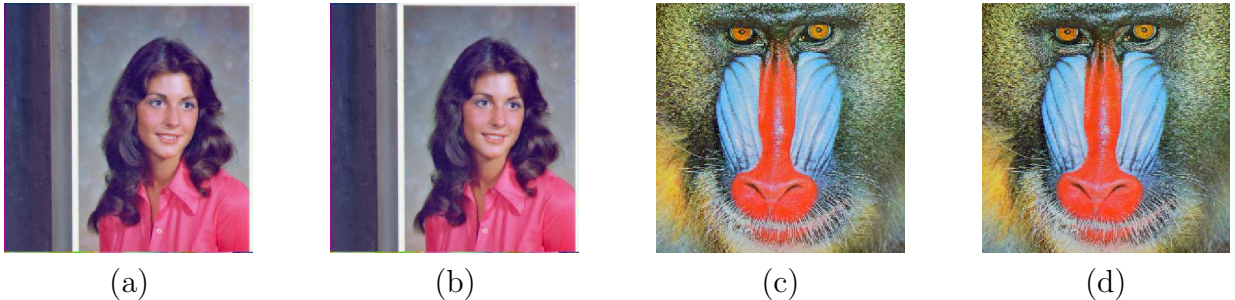


Figure 3: (a) and (c): Original images; (b) and (d): Reconstructed images.

Note that QPR processes three channels in a holistic manner, which seems to be more suitable methodology compared with the channel-by-channel real method, see [50]. We remark that low-rank phase retrieval that utilizes the low-rankness to aid the phaseless recovery has recently been studied (e.g., [33, 42, 59]). Noting that (color) images are approximately low-rank, we thus believe the advantage of quaternion-based method can be further illustrated via numerical examples when the low-rankness is incorporated, just like previous works in image restoration [17] and inpainting [13, 31].

⁵<https://sipi.usc.edu/database/database.php?volume=misc&image=4#top>

5.3 Variants of Quaternion Wirtinger Flow

In this part, we compare the empirical success rate of QWF, QTWF, QTAF under $\frac{n}{d} = 3 : 0.5 : 13$, and the underlying $\mathbf{x} \in \mathbb{Q}^{50}$ is randomly drawn as previous experiments. Each success rate is based on 100 independent trials, and we use 100 power iterations for initialization, followed by 1500 updates. For QWF we set $\eta = 0.2$. For QTWF and QTAF introduced in Appendix B, the parameters are tuned to be well functioning. Specifically, we set $(\theta_z^{lb}, \theta_z^{ub}, \theta_h, \theta_y, \eta) = (0.3, 4.5, 5, 3, 0.8)$ for QTWF, $(\gamma, \rho, \eta) = (0.8, \frac{1}{6}, 1.2)$ for QTAF. The results are shown in Figure 4. Evidently, at the cost of more parameters and more complicated algorithms, QTWF and QTAF perform notably better than QWF. In addition, it is similar to incorporate the pure quaternion priori into QTWF and QTAF, thus no further exposition will be given here.

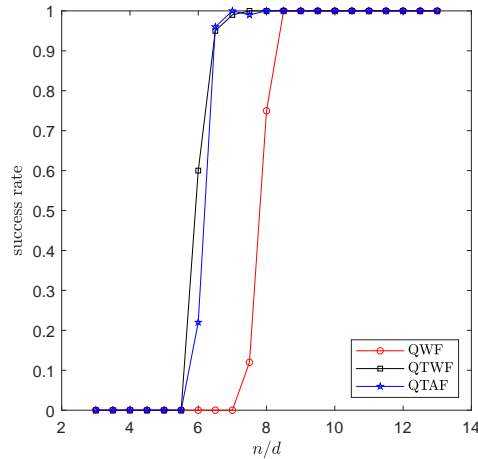


Figure 4: Success rate of QWF, QTWF, QTAF under different sample sizes.

6 Concluding Remarks

Compared with the traditional signal processing in the real or complex field, quaternion-based techniques process signals over the quaternion algebra \mathbb{Q} , which has been observed to be beneficial in a bunch of applications. On the other hand, phase retrieval refers to the phases signal recovery that arises when the sensor fails to capture the phase, probably due to the prohibitive cost or the bad circumstance. Independently, these two fields have been developed fairly well, but the study of quaternion phase retrieval is yet to open. To the best of our knowledge, the only related result is due to [16], but restricted to real measurement matrix. Specifically, even the identifiability question of fundamental importance, i.e., to what extent the signal can be reconstructed if the measurement matrix is quaternionic, remains unclear. Since quaternion signal processing and phase retrieval naturally intersect in color imaging problems, this is a gap in previous research.

In this paper, we initiate the study of quaternion phase retrieval (QPR) problem, which is formulated as the reconstruction of $\mathbf{x} \in \mathbb{Q}^d$ from $|\mathbf{A}\mathbf{x}|^2$ with known $\mathbf{A} \in \mathbb{Q}^{n \times d}$. As the theoretical foundation, we first confirm via Mendelson's small ball method that, the global right quaternion phase factor is the only trivial ambiguity. This suggests our goal is to recover $\{\mathbf{x}q : |q| = 1\}$, and the natural error metric is $\text{dist}(\mathbf{z}, \mathbf{x}) = \min_{|q|=1} |\mathbf{x} - \mathbf{z}q|$. Then, we propose quaternion Wirtinger flow (QWF) as a scalable and practical algorithm for solving QPR. The

linear convergence of QWF has been proved and presented as a main theoretical result. The technical ingredients involve the HR calculus and many techniques for handling quaternion matrices. While our proof strategy is adjusted from the complex Wirtinger flow [9], a series of different treatments is employed with some new machinery, see our discussions in Remark 2, 6.

Besides, extra attention has been paid to pure quaternion signal $\mathbf{x} \in \mathbb{Q}_p^d$. Fortunately, with the additional minor assumption that $\mathcal{P}^i(\mathbf{x}), \mathcal{P}^j(\mathbf{x}), \mathcal{P}^k(\mathbf{x})$ are real linearly independent, it becomes possible to recover \mathbf{x} up to a sign. Accordingly, the error measure changes to $\text{dist}_p(\mathbf{z}, \mathbf{x}) = \min\{\|\mathbf{z} + \mathbf{x}\|, \|\mathbf{z} - \mathbf{x}\|\}$. Moreover, we propose a variant of QWF (PQWF) that embeds a phase factor estimate (4.1) into the iteration. Theoretically, the obtained sequence linearly converges to \mathbf{x} up to a sign; Experimentally, such modification can effectively utilize the pure quaternion constraint and enjoys earlier phase transition (Figure 2). Noting that TWF [15] and TAF [62] are two representatives among refinements of WF, we also numerically test the performances of QTWF and QTAF. As it turns out, they can still deliver notable improvements in QPR (Figure 4).

While we hope this work can provide a starting point for the research of QPR and describe a new quaternion signal recovery model for application, there are undoubtedly many questions worth further exploration. Here, we point out two to close this paper. Firstly, although $O(d)$ measurements have been shown to be sufficient for QPR, it would be of theoretical interest to investigate the precise measurement number needed for recovery of all signals in \mathbb{Q}^d . This is known as the minimal measurement number in phase retrieval (e.g., [2, 3, 18, 64]), for which algebraic geometry usually serves as a main tool. Secondly, compared to $\mathbf{A} \sim \mathcal{N}_{\mathbb{Q}}^{n \times d}$, coded diffraction pattern (CDP) that applies Fourier transform to the masked signal would be more practical for some real-world applications, see [8] for instance. It is thus appealing to develop a similar measurement ensemble for quaternion signal. This direction may be fruitful since unlike the classical Fourier transform, the quaternion one is more flexible in the choice of the transform axis, which is described by a unit pure quaternion.

References

- [1] A. BADEŃSKA AND Ł. BŁASZCZYK, *Compressed sensing for real measurements of quaternion signals*, Journal of the Franklin Institute, 354 (2017), pp. 5753–5769.
- [2] R. BALAN, P. CASAZZA, AND D. EDIDIN, *On signal reconstruction without phase*, Applied and Computational Harmonic Analysis, 20 (2006), pp. 345–356.
- [3] A. S. BANDEIRA, J. CAHILL, D. G. MIXON, AND A. A. NELSON, *Saving phase: Injectivity and stability for phase retrieval*, Applied and Computational Harmonic Analysis, 37 (2014), pp. 106–125.
- [4] P. BAS, N. LE BIHAN, AND J.-M. CHASSERY, *Color image watermarking using quaternion Fourier transform*, in 2003 IEEE International Conference on Acoustics, Speech, and Signal Processing, 2003. Proceedings.(ICASSP'03)., vol. 3, IEEE, 2003, pp. III–521.
- [5] E. BAYRO-CORROCHANO, *The theory and use of the quaternion wavelet transform*, Journal of Mathematical Imaging and Vision, 24 (2006), pp. 19–35.

- [6] V. BENTKUS, *An inequality for tail probabilities of martingales with differences bounded from one side*, Journal of Theoretical Probability, 16 (2003), pp. 161–173.
- [7] O. BUNK, A. DIAZ, F. PFEIFFER, C. DAVID, B. SCHMITT, D. K. SATAPATHY, AND J. F. VAN DER VEEN, *Diffraction imaging for periodic samples: retrieving one-dimensional concentration profiles across microfluidic channels*, Acta Crystallographica Section A: Foundations of Crystallography, 63 (2007), pp. 306–314.
- [8] E. J. CANDÈS, Y. C. ELDAR, T. STROHMER, AND V. VORONINSKI, *Phase retrieval via matrix completion*, SIAM review, 57 (2015), pp. 225–251.
- [9] E. J. CANDÈS, X. LI, AND M. SOLTANOLKOTABI, *Phase retrieval via Wirtinger flow: Theory and algorithms*, IEEE Transactions on Information Theory, 61 (2015), pp. 1985–2007.
- [10] E. J. CANDÈS, T. STROHMER, AND V. VORONINSKI, *Phaselift: Exact and stable signal recovery from magnitude measurements via convex programming*, Communications on Pure and Applied Mathematics, 66 (2013), pp. 1241–1274.
- [11] B. CHEN, H. SHU, G. COATRIEUX, G. CHEN, X. SUN, AND J. L. COATRIEUX, *Color image analysis by quaternion-type moments*, Journal of mathematical imaging and vision, 51 (2015), pp. 124–144.
- [12] B. CHEN, H. SHU, H. ZHANG, G. CHEN, C. TOUMOULIN, J.-L. DILLENSEGER, AND L. LUO, *Quaternion Zernike moments and their invariants for color image analysis and object recognition*, Signal processing, 92 (2012), pp. 308–318.
- [13] J. CHEN AND M. K. NG, *Color image inpainting via robust pure quaternion matrix completion: Error bound and weighted loss*, SIAM Journal on Imaging Sciences, 15 (2022), pp. 1469–1498.
- [14] J. CHEN AND M. K. NG, *Error bound of empirical ℓ_2 risk minimization for noisy standard and generalized phase retrieval problems*, arXiv preprint arXiv:2205.13827, (2022).
- [15] Y. CHEN AND E. J. CANDÈS, *Solving random quadratic systems of equations is nearly as easy as solving linear systems*, Communications on pure and applied mathematics, 70 (2017), pp. 822–883.
- [16] Y. CHEN, C. CHENG, AND Q. SUN, *Phase retrieval of complex and vector-valued functions*, Journal of Functional Analysis, 283 (2022), p. 109593.
- [17] Y. CHEN, X. XIAO, AND Y. ZHOU, *Low-rank quaternion approximation for color image processing*, IEEE Transactions on Image Processing, 29 (2019), pp. 1426–1439.
- [18] A. CONCA, D. EDIDIN, M. HERING, AND C. VINZANT, *An algebraic characterization of injectivity in phase retrieval*, Applied and Computational Harmonic Analysis, 38 (2015), pp. 346–356.
- [19] S. DIRKSEN, G. LECUÉ, AND H. RAUHUT, *On the gap between restricted isometry properties and sparse recovery conditions*, IEEE Transactions on Information Theory, 64 (2016), pp. 5478–5487.

- [20] T. A. ELL AND S. J. SANGWINE, *Hypercomplex Fourier transforms of color images*, IEEE Transactions on image processing, 16 (2006), pp. 22–35.
- [21] C. FIENUP AND J. DAINTY, *Phase retrieval and image reconstruction for astronomy*, Image recovery: theory and application, 231 (1987), p. 275.
- [22] J. R. FIENUP, *Reconstruction of an object from the modulus of its Fourier transform*, Optics letters, 3 (1978), pp. 27–29.
- [23] J. R. FIENUP, *Phase retrieval algorithms: a comparison*, Applied optics, 21 (1982), pp. 2758–2769.
- [24] P. FLETCHER AND S. J. SANGWINE, *The development of the quaternion wavelet transform*, Signal Processing, 136 (2017), pp. 2–15.
- [25] S. FOUCART AND H. RAUHUT, *A mathematical introduction to compressive sensing*, Springer, 2013.
- [26] S. GAI, G. YANG, M. WAN, AND L. WANG, *Denoising color images by reduced quaternion matrix singular value decomposition*, Multidimensional Systems and Signal Processing, 26 (2015), pp. 307–320.
- [27] C. J. GAUDET AND A. S. MAIDA, *Deep quaternion networks*, in 2018 International Joint Conference on Neural Networks (IJCNN), IEEE, 2018, pp. 1–8.
- [28] R. W. GERCHBERG, *A practical algorithm for the determination of plane from image and diffraction pictures*, Optik, 35 (1972), pp. 237–246.
- [29] C. HUANG, M. K. NG, T. WU, AND T. ZENG, *Quaternion-based dictionary learning and saturation-value total variation regularization for color image restoration*, IEEE Transactions on Multimedia, 24 (2021), pp. 3769–3781.
- [30] M. HUANG AND Z. XU, *Performance bound of the intensity-based model for noisy phase retrieval*, arXiv preprint arXiv:2004.08764, (2020).
- [31] Z. JIA, M. K. NG, AND G.-J. SONG, *Robust quaternion matrix completion with applications to image inpainting*, Numerical Linear Algebra with Applications, 26 (2019), p. e2245.
- [32] N. LE BIHAN AND S. J. SANGWINE, *Quaternion principal component analysis of color images*, in Proceedings 2003 International Conference on Image Processing (Cat. No. 03CH37429), vol. 1, IEEE, 2003, pp. I–809.
- [33] K. LEE, S. BAHMANI, Y. C. ELДАР, AND J. ROMBERG, *Phase retrieval of low-rank matrices by anchored regression*, Information and Inference: A Journal of the IMA, 10 (2021), pp. 285–332.
- [34] Y. LI, M. WEI, F. ZHANG, AND J. ZHAO, *On the power method for quaternion right eigenvalue problem*, Journal of Computational and Applied Mathematics, 345 (2019), pp. 59–69.

- [35] D. P. MANDIC, C. JAHANCHAH, AND C. C. TOOK, *A quaternion gradient operator and its applications*, IEEE Signal Processing Letters, 18 (2010), pp. 47–50.
- [36] S. MENDELSON, *Learning without concentration*, Journal of the ACM (JACM), 62 (2015), pp. 1–25.
- [37] S. MENDELSON, *Learning without concentration for general loss functions*, Probability Theory and Related Fields, 171 (2018), pp. 459–502.
- [38] J. MIAO, T. ISHIKAWA, Q. SHEN, AND T. EARNEST, *Extending x-ray crystallography to allow the imaging of noncrystalline materials, cells, and single protein complexes*, Annual review of physical chemistry, 59 (2008), pp. 387–410.
- [39] J. MIAO AND K. I. KOU, *Quaternion-based bilinear factor matrix norm minimization for color image inpainting*, IEEE Transactions on Signal Processing, 68 (2020), pp. 5617–5631.
- [40] J. MIAO AND K. I. KOU, *Color image recovery using low-rank quaternion matrix completion algorithm*, IEEE Transactions on Image Processing, 31 (2021), pp. 190–201.
- [41] R. P. MILLANE, *Phase retrieval in crystallography and optics*, JOSA A, 7 (1990), pp. 394–411.
- [42] S. NAYER, P. NARAYANAMURTHY, AND N. VASWANI, *Provable low rank phase retrieval*, IEEE Transactions on Information Theory, 66 (2020), pp. 5875–5903.
- [43] Y. NESTEROV, *Introductory lectures on convex optimization: A basic course*, vol. 87, Springer Science & Business Media, 2003.
- [44] P. NETRAPALLI, P. JAIN, AND S. SANGHAVI, *Phase retrieval using alternating minimization*, Advances in Neural Information Processing Systems, 26 (2013).
- [45] T. PARCOLLET, M. MORCHID, AND G. LINARÈS, *Quaternion convolutional neural networks for heterogeneous image processing*, in ICASSP 2019-2019 IEEE International Conference on Acoustics, Speech and Signal Processing (ICASSP), IEEE, 2019, pp. 8514–8518.
- [46] S.-C. PEI AND C.-M. CHENG, *A novel block truncation coding of color images using a quaternion-moment-preserving principle*, IEEE Transactions on Communications, 45 (1997), pp. 583–595.
- [47] S.-C. PEI AND C.-M. CHENG, *Color image processing by using binary quaternion-moment-preserving thresholding technique*, IEEE Transactions on Image Processing, 8 (1999), pp. 614–628.
- [48] L. RABINER AND B.-H. JUANG, *Fundamentals of speech recognition*, Prentice-Hall, Inc., 1993.
- [49] H. REICHENBACH, *Philosophic foundations of quantum mechanics*, Courier Corporation, 1998.

- [50] S. J. SANGWINE, *Fourier transforms of colour images using quaternion or hypercomplex numbers*, Electronics letters, 32 (1996), pp. 1979–1980.
- [51] Y. SHECHTMAN, Y. C. ELДАР, O. COHEN, H. N. CHAPMAN, J. MIAO, AND M. SEGEV, *Phase retrieval with application to optical imaging: a contemporary overview*, IEEE signal processing magazine, 32 (2015), pp. 87–109.
- [52] L. SHI AND B. FUNT, *Quaternion color texture segmentation*, Computer Vision and image understanding, 107 (2007), pp. 88–96.
- [53] M. SOLTANOLKOTABI, *Algorithms and theory for clustering and nonconvex quadratic programming*, Stanford University, 2014.
- [54] G. SONG, W. DING, AND M. K. NG, *Low rank pure quaternion approximation for pure quaternion matrices*, SIAM Journal on Matrix Analysis and Applications, 42 (2021), pp. 58–82.
- [55] Ö. N. SUBAKAN AND B. C. VEMURI, *A quaternion framework for color image smoothing and segmentation*, International Journal of Computer Vision, 91 (2011), pp. 233–250.
- [56] C. C. TOOK AND D. P. MANDIC, *The quaternion lms algorithm for adaptive filtering of hypercomplex processes*, IEEE Transactions on Signal Processing, 57 (2008), pp. 1316–1327.
- [57] C. C. TOOK AND D. P. MANDIC, *A quaternion widely linear adaptive filter*, IEEE Transactions on Signal Processing, 58 (2010), pp. 4427–4431.
- [58] B. C. UJANG, C. C. TOOK, AND D. P. MANDIC, *Quaternion-valued nonlinear adaptive filtering*, IEEE Transactions on Neural Networks, 22 (2011), pp. 1193–1206.
- [59] N. VASWANI, S. NAYER, AND Y. C. ELДАР, *Low-rank phase retrieval*, IEEE Transactions on Signal Processing, 65 (2017), pp. 4059–4074.
- [60] R. VERSHYNIN, *High-dimensional probability: An introduction with applications in data science*, vol. 47, Cambridge university press, 2018.
- [61] A. WALTHER, *The question of phase retrieval in optics*, Optica Acta: International Journal of Optics, 10 (1963), pp. 41–49.
- [62] G. WANG, G. B. GIANNAKIS, AND Y. C. ELДАР, *Solving systems of random quadratic equations via truncated amplitude flow*, IEEE Transactions on Information Theory, 64 (2017), pp. 773–794.
- [63] X.-Y. WANG, C.-P. WANG, H.-Y. YANG, AND P.-P. NIU, *A robust blind color image watermarking in quaternion Fourier transform domain*, Journal of Systems and Software, 86 (2013), pp. 255–277.
- [64] Y. WANG AND Z. XU, *Generalized phase retrieval: measurement number, matrix recovery and beyond*, Applied and Computational Harmonic Analysis, 47 (2019), pp. 423–446.
- [65] D. XU, C. JAHANCHAH, C. C. TOOK, AND D. P. MANDIC, *Enabling quaternion derivatives: the generalized hr calculus*, Royal Society open science, 2 (2015), p. 150255.

- [66] D. XU AND D. P. MANDIC, *The theory of quaternion matrix derivatives*, IEEE Transactions on Signal Processing, 63 (2015), pp. 1543–1556.
- [67] D. XU, Y. XIA, AND D. P. MANDIC, *Optimization in quaternion dynamic systems: Gradient, hessian, and learning algorithms*, IEEE transactions on neural networks and learning systems, 27 (2015), pp. 249–261.
- [68] F. ZHANG, *Quaternions and matrices of quaternions*, Linear algebra and its applications, 251 (1997), pp. 21–57.
- [69] X. ZHU, Y. XU, H. XU, AND C. CHEN, *Quaternion convolutional neural networks*, in Proceedings of the European Conference on Computer Vision (ECCV), 2018, pp. 631–647.

A Auxiliary Results

Small ball method due to Mendelson [36,37] is an effective tool to lower bound a non-negative empirical process. The version provided below can be found in Lemma 1 of [19] (with $p = 2$).

Lemma 7. (Mendelson’s Small Ball Method) *Assume \mathcal{F} be a class of functions from \mathbb{C}^n into \mathbb{C} . Let $\boldsymbol{\varphi}$ be random vector on \mathbb{C}^n , and $\boldsymbol{\varphi}_1, \dots, \boldsymbol{\varphi}_m$ be independent copies of $\boldsymbol{\varphi}$. For $u > 0$ we define $Q_{\mathcal{F}}(u) = \inf_{f \in \mathcal{F}} \mathbb{P}(|f(\boldsymbol{\varphi})| \geq u)$. Let $\varepsilon_1, \dots, \varepsilon_n$ be independent Rademacher random variables (i.e., $\mathbb{P}(\varepsilon_k = 1) = \mathbb{P}(\varepsilon_k = -1) = 1/2$), we further define $R_m(\mathcal{F}) = \mathbb{E} \sup_{f \in \mathcal{F}} |\frac{1}{m} \sum_{k=1}^m \varepsilon_k f(\boldsymbol{\varphi}_k)|$. Then, for any $u > 0$, $t > 0$, with probability at least $1 - 2 \exp(-2t^2)$, we have*

$$\inf_{f \in \mathcal{F}} \frac{1}{m} \sum_{k=1}^m |f(\boldsymbol{\varphi}_k)|^2 \geq u^2 \left(Q_{\mathcal{F}}(2u) - \frac{4}{u} R_m(\mathcal{F}) - \frac{t}{\sqrt{m}} \right). \quad (\text{A.1})$$

We provide some expectation results to support our proof.

Lemma 8. *Assume entries of $\boldsymbol{\alpha} \in \mathbb{Q}^d$ are i.i.d. drawn from $\mathcal{N}_{\mathbb{Q}}$, and $\mathbf{u}, \mathbf{v} \in \mathbb{Q}^d$ satisfy $\|\mathbf{u}\| = \|\mathbf{v}\| = 1$. Then we have the following:*

- (a) (rotational invariance) *For any unitary matrix $\mathbf{P} \in \mathbb{Q}^{d \times d}$, $\mathbf{P}\boldsymbol{\alpha}$ and $\boldsymbol{\alpha}$ have the same distribution.*
- (b) $\mathbb{E}|\boldsymbol{\alpha}^* \mathbf{u}|^{2l} = \frac{(l+1)!}{2^l}$ *for any positive integer l .*
- (c) $\mathbb{E}[\Re(\mathbf{u}^* \boldsymbol{\alpha} \boldsymbol{\alpha}^* \mathbf{v})]^2 = \frac{1}{4} + \frac{5}{4}[\Re(\mathbf{u}^* \mathbf{v})]^2 - \frac{1}{4}|\Im(\mathbf{u}^* \mathbf{v})|^2$.
- (d) $\mathbb{E}[\boldsymbol{\alpha} \boldsymbol{\alpha}^* \mathbf{u} | \boldsymbol{\alpha}^* \mathbf{v}|^2] = \mathbf{u} + \frac{1}{2} \mathbf{v} \mathbf{v}^* \mathbf{u}$.

Proof. (a) Recalling the definition of $\mathcal{T}_1(\cdot)$ below (2.4), we only need to show $\mathcal{T}_1(\mathbf{P}\boldsymbol{\alpha})$ and $\mathcal{T}_1(\boldsymbol{\alpha})$ have the same distribution. Noting $\mathcal{T}_1(\mathbf{P}\boldsymbol{\alpha}) = \mathcal{T}(\mathbf{P})\mathcal{T}_1(\boldsymbol{\alpha})$, and observe that $\mathcal{T}_1(\boldsymbol{\alpha})$ has entries i.i.d. drawn from $\frac{1}{2}\mathcal{N}(0, 1)$, while $\mathcal{T}(\mathbf{P})$ is real orthogonal matrix. By rotational invariance of real Gaussian vector, the result is immediate.

(b) By rotation invariance, $\boldsymbol{\alpha}^* \mathbf{u}$ is a realization of $\mathcal{N}_{\mathbb{Q}}$, hence $4|\boldsymbol{\alpha}^* \mathbf{u}|^2$ is just the χ^2 distribution with 4 degrees of freedom. Hence, the result follows known moment result of χ^2 distribution.

(c) We find a unitary \mathbf{P} such that $\mathbf{P}\mathbf{u} = \mathbf{e}_1$, further write $\mathbf{P}\mathbf{v} = \mathbf{w} = [w_i]$, $\mathbf{P}\boldsymbol{\alpha} = \boldsymbol{\gamma} = [\gamma_i]$, where $\boldsymbol{\gamma}$ and $\boldsymbol{\alpha}$ have the same distribution. Some algebra gives

$$\begin{aligned}\mathbb{E}[\Re(\mathbf{u}^* \boldsymbol{\alpha} \boldsymbol{\alpha}^* \mathbf{v})]^2 &= \mathbb{E}[\Re(\mathbf{e}_1^\top \boldsymbol{\gamma} \boldsymbol{\gamma}^* \mathbf{w})]^2 = \mathbb{E}[|\gamma_1|^2 \Re(w_1) + \Re(\gamma_1 \sum_{k=2}^d \bar{\gamma}_k w_k)]^2 \\ &= \mathbb{E}[|\gamma_1|^2 \Re(w_1) + \sqrt{1 - |w_1|^2} \cdot \Re(\gamma_1 \tilde{\gamma})]^2 = [\Re(w_1)]^2 \mathbb{E}|\gamma_1|^4 + (1 - |w_1|^2) \mathbb{E}[\Re(\gamma_1 \tilde{\gamma})]^2 \\ &= \frac{3}{2} [\Re(w_1)]^2 + \frac{1}{4} (1 - |w_1|^2) = \frac{1}{4} + \frac{5}{4} [\Re(\mathbf{u}^* \mathbf{v})]^2 - \frac{1}{4} |\Im(\mathbf{u}^* \mathbf{v})|^2,\end{aligned}$$

where we let $\tilde{\gamma} = \sum_{k=2}^d w_k \bar{\gamma}_k / \sqrt{1 - |w_1|^2}$ in the second line, and invoke the fact that $\tilde{\gamma}, \gamma_1$ are independent copies of $\mathcal{N}_{\mathbb{Q}}$.

(d) We similarly find unitary \mathbf{P} such that $\mathbf{P}\mathbf{v} = \mathbf{e}_1$, and denote $\mathbf{P}\mathbf{u} = \mathbf{w}$, $\mathbf{P}\boldsymbol{\alpha} = \boldsymbol{\gamma} = [\gamma_i]$. Note that $\boldsymbol{\gamma}$ and $\boldsymbol{\alpha}$ have the same distribution. Then, it proceeds that

$$\begin{aligned}\mathbb{E}[\boldsymbol{\alpha} \boldsymbol{\alpha}^* \mathbf{u} | \boldsymbol{\alpha}^* \mathbf{v}]^2 &= \mathbb{E}[\mathbf{P}^* \boldsymbol{\gamma} \boldsymbol{\gamma}^* \mathbf{w} | \boldsymbol{\gamma}^* \mathbf{e}_1]^2 = \mathbf{P}^* [\mathbb{E}|\gamma_1|^2 \boldsymbol{\gamma} \boldsymbol{\gamma}^*] \mathbf{w} \\ &= \mathbf{P}^* \left[\frac{1}{2} \mathbf{e}_1 \mathbf{e}_1^* + \mathbf{I}_d \right] \mathbf{w} = \left(\mathbf{I}_d + \frac{1}{2} \mathbf{v} \mathbf{v}^* \right) \mathbf{u},\end{aligned}$$

the result follows. \square

Proof of Lemma 1. We only prove $t = 0$ for (3.11), for general t the result follows by noting \mathbf{z}_t remains in $E_\epsilon(\mathbf{x})$. We do some estimates as follows

$$\begin{aligned}\text{dist}^2(\mathbf{z}_1, \mathbf{x}) &\leq \|\mathbf{z}_0 - \eta \nabla f(\mathbf{z}_0) - \mathbf{x} \phi(\mathbf{z}_0)\|^2 \\ &= \text{dist}^2(\mathbf{z}_0, \mathbf{x}) + \eta^2 \|\nabla f(\mathbf{z}_0)\|^2 - 2\eta \cdot \Re \langle \nabla f(\mathbf{z}_0), \mathbf{z}_0 - \mathbf{x} \phi(\mathbf{z}_0) \rangle \\ &\leq \left(1 - \frac{2\eta}{\tau}\right) \text{dist}^2(\mathbf{z}_0, \mathbf{x}) + \eta \left(\eta - \frac{2}{\beta}\right) \|\nabla f(\mathbf{z}_0)\|^2 \leq \left(1 - \frac{2\eta}{\tau}\right) \text{dist}^2(\mathbf{z}_0, \mathbf{x}),\end{aligned}$$

where we plug in (3.10) in the third line. \square

Proof of Lemma 4. Recall that $\mathbf{z}_0 = \left(\frac{1}{n} \sum_{k=1}^n |\boldsymbol{\alpha}_k^* \mathbf{x}|^2\right)^{1/2} \cdot \boldsymbol{\nu}_{in}$ (where $\|\boldsymbol{\nu}_{in}\| = 1$ is the eigenvector of \mathbf{S}_{in} (3.7) corresponding to the largest standard eigenvalue), and so

$$\begin{aligned}\text{dist}(\mathbf{z}_0, \mathbf{x}) &= \|\mathbf{z}_0 - \mathbf{x} \phi(\boldsymbol{\nu}_{in})\| \leq \|\mathbf{z}_0 - \boldsymbol{\nu}_{in}\| + \|\boldsymbol{\nu}_{in} - \mathbf{x} \phi(\boldsymbol{\nu}_{in})\| \\ &\leq \left| \frac{1}{n} \sum_{k=1}^n |\boldsymbol{\alpha}_k^* \mathbf{x}|^2 - 1 \right|^{1/2} + \sqrt{2} \sqrt{1 - |\boldsymbol{\nu}_{in}^* \mathbf{x}|} := T_1 + \sqrt{2} T_2.\end{aligned}$$

Bernstein's inequality gives $\mathbb{P}(|T_1|^2 \geq t) \leq 2 \exp(-cn \min\{t, t^2\})$ for any $t > 0$. Taking $t = \frac{\delta}{4}$, then with probability at least $1 - 2 \exp(-c\delta^2 n/16)$, $T_1 \leq \frac{\delta}{2}$.

We then go into T_2 . Similar to the proof of Lemma 3, specifically using the real representation of a quaternion matrix and Lemma 9, we can show with probability at least $1 - C_1 n^{-9} - C_2 \exp(-C_3 d)$, $\|\mathbf{S}_{in} - \mathbb{E} \mathbf{S}_{in}\| = \|\mathbf{S}_{in} - \mathbf{I}_d - \frac{1}{2} \mathbf{x} \mathbf{x}^*\| \leq \frac{\delta}{16}$. Therefore, we have $\frac{\delta}{16} \geq \boldsymbol{\nu}_{in}^* \mathbf{S}_{in} \boldsymbol{\nu}_{in} - 1 - \frac{1}{2} |\boldsymbol{\nu}_{in}^* \mathbf{x}|^2$, and $\frac{\delta}{16} \geq \frac{3}{2} - \mathbf{x}^* \mathbf{S}_{in} \mathbf{x}$. By construction $\boldsymbol{\nu}_{in}^* \mathbf{S}_{in} \boldsymbol{\nu}_{in} \geq \mathbf{x}^* \mathbf{S}_{in} \mathbf{x}$. Taken collectively, it gives $\frac{\delta}{16} \geq \frac{1}{2} - \frac{\delta}{16} - \frac{1}{2} |\boldsymbol{\nu}_{in}^* \mathbf{x}|^2 \geq \frac{1}{2} (1 - |\boldsymbol{\nu}_{in}^* \mathbf{x}|) - \frac{\delta}{16}$, hence $T_2 \leq \frac{\delta}{2}$. The proof is concluded. \square

Lemma 9. Assume $\gamma_1, \dots, \gamma_n$ are independent random vectors in \mathbb{R}^d that have entries $[\gamma_{kj}]$ i.i.d. drawn from $\mathcal{N}(0, 1)$. Fix $i, j \in \{1, 2\}$ and any sufficiently small $\delta > 0$, when $n \geq C_1 \delta^{-2} d \log n$ for sufficiently large C_1 , with probability at least $1 - 2n^{-9} - 2 \exp(-cd)$, we have

$$\left\| \frac{1}{n} \sum_{k=1}^n \gamma_{ki} \gamma_{kj} \gamma_k \gamma_k^\top - \mathbb{E}[\gamma_{ki} \gamma_{kj} \gamma_k \gamma_k^\top] \right\| \leq C\delta.$$

Proof. We only deal with $i \neq j$, specifically $i = 1, j = 2$, since the proof for $i = j$ is parallel and involve simpler calculations. We define the event $\mathcal{A} = \{\max_{k \in [n]} \max_{i=1,2} |\gamma_{ki}| \leq \zeta := C_1 \sqrt{\log n}\}$. A standard estimate gives that we can pick some C_1 such that $\mathbb{P}(\mathcal{A}) \geq \mathbb{P}(|\gamma_{ki}| \leq \zeta) \geq 1 - n^{-9}$ (e.g., Proposition 4, [13]). Conditional on \mathcal{A} , we define the random variables $\tilde{\gamma}_{ki}, k \in [n], j \in [2]$ that follow the conditional distribution of γ_{ki} . Evidently, $\tilde{\gamma}_{ki}$ possesses the p.d.f. $\frac{\tilde{c}}{\sqrt{2\pi}} \exp(-\frac{x^2}{2}) \mathbb{1}(|x| \leq \zeta)$, where $\tilde{c} \in (1, \frac{1}{1-n^{-9}})$ is the normalization constant. Writing $\tilde{\gamma}_k = [\tilde{\gamma}_{k1}, \tilde{\gamma}_{k2}, \dots, \tilde{\gamma}_{kd}]^\top$, we proceed by conditioning on the event \mathcal{A} , hence we need to show with high probability $T \leq C\delta$, with T defined and then estimated as

$$\begin{aligned} T &:= \left\| \frac{1}{n} \sum_{k=1}^n \tilde{\gamma}_{k1} \tilde{\gamma}_{k2} \tilde{\gamma}_k \tilde{\gamma}_k^\top - \mathbb{E}[\gamma_{k1} \gamma_{k2} \gamma_k \gamma_k^\top] \right\| \leq \left\| \frac{1}{n} \sum_{k=1}^n \tilde{\gamma}_{k1} \tilde{\gamma}_{k2} \tilde{\gamma}_k \tilde{\gamma}_k^\top - \mathbb{E}[\tilde{\gamma}_{k1} \tilde{\gamma}_{k2} \tilde{\gamma}_k \tilde{\gamma}_k^\top] \right\| \\ &\quad + \left\| \mathbb{E}[\tilde{\gamma}_{k1} \tilde{\gamma}_{k2} \tilde{\gamma}_k \tilde{\gamma}_k^\top] - \mathbb{E}[\gamma_{k1} \gamma_{k2} \gamma_k \gamma_k^\top] \right\| := T_{11} + T_{12}. \end{aligned} \quad (\text{A.2})$$

We estimate T_{12} first. A simple observation is that all but (1, 2)-th, (2, 1)-th entries of $\mathbb{E}[\tilde{\gamma}_{k1} \tilde{\gamma}_{k2} \tilde{\gamma}_k \tilde{\gamma}_k^\top]$, $\mathbb{E}[\gamma_{k1} \gamma_{k2} \gamma_k \gamma_k^\top]$ are zero, and the (1, 2)-th, (2, 1)-th entry can be estimated as

$$\begin{aligned} |\mathbb{E}\tilde{\gamma}_{k1}^2 \mathbb{E}\tilde{\gamma}_{k2}^2 - \mathbb{E}\gamma_{k1}^2 \mathbb{E}\gamma_{k2}^2| &\leq |\mathbb{E}\tilde{\gamma}_{k2}^2 (\mathbb{E}\gamma_{k1}^2 - \mathbb{E}\tilde{\gamma}_{k1}^2)| + |\mathbb{E}\gamma_{k1}^2 (\mathbb{E}\tilde{\gamma}_{k2}^2 - \mathbb{E}\gamma_{k2}^2)| \\ &\leq 4|\mathbb{E}\gamma_{k1}^2 - \mathbb{E}\tilde{\gamma}_{k1}^2| = 4((\tilde{c}^2 - 1)\mathbb{E}\gamma_{k1}^2 + 2 \int_{\zeta}^{\infty} \frac{x^2}{\sqrt{2\pi}} \exp(-\frac{x^2}{2}) dx) \\ &\leq 4(3(\tilde{c} - 1) + \int_{\zeta}^{\infty} \frac{x^3}{\zeta} \exp(-\frac{x^2}{2}) dx) = \frac{12}{n^9 - 1} + \frac{8}{\zeta} \left(\frac{\zeta^2}{2} + 1\right) \exp(-\frac{\zeta^2}{2}) < \delta. \end{aligned}$$

In the last inequality we plug in $\zeta = C_1 \sqrt{\log n}$ and then can see it holds under a $n \geq \delta^{-2}$ and slightly large C_1 . Thus, we obtain $T_{12} \leq 2\delta$. We construct \mathcal{N}_1 as a $\frac{1}{4}$ -net of \mathbb{S}^{d-1} (unit Euclidean sphere of \mathbb{R}^d), and we can assume $|\mathcal{N}| \leq 9^d$. A standard covering argument gives (e.g., Chapter 4.1.1, [60])

$$T_{11} \leq 2 \sup_{\mathbf{u} \in \mathcal{N}_1} \sup_{\mathbf{v} \in \mathcal{N}_1} \left| \frac{1}{n} \sum_{k=1}^n \gamma_{ki} \gamma_{kj} (\mathbf{u}^\top \gamma_k) (\mathbf{v}^\top \gamma_k) - \mathbb{E}[\gamma_{ki} \gamma_{kj} (\mathbf{u}^\top \gamma_k) (\mathbf{v}^\top \gamma_k)] \right| := 2\hat{T}_{11}. \quad (\text{A.3})$$

One can also estimate the sub-exponential norm $\|\cdot\|_{\psi_1}$ by using Lemma 2.7.7, [60]

$$\|\gamma_{ki} \gamma_{kj} (\mathbf{u}^\top \gamma_k) (\mathbf{v}^\top \gamma_k)\|_{\psi_1} \leq \zeta^2 \|\mathbf{u}^\top \gamma_k\|_{\psi_2} \|\mathbf{v}^\top \gamma_k\|_{\psi_2} \leq C_2 \log n.$$

So, we can invoke Bernstein's inequality (Theorem 2.8.1, [60]) for fixed \mathbf{u}, \mathbf{v} , then a union bound over $\mathbf{u}, \mathbf{v} \in \mathcal{N}_1$ yields for some c ,

$$\mathbb{P}(\hat{T}_{11} \geq t) \leq 2 \exp\left(-c \cdot \left(\frac{n}{\log n}\right) \min\{t, t^2\} + (4 \log 3)d\right), \quad \forall t > 0. \quad (\text{A.4})$$

Taking $t = \delta$, it delivers that, as long as $n \geq C_3 \delta^{-2} d \log n$, with probability at least $1 - 2 \exp(-\Omega(d))$ we have $\widehat{T}_{11} \leq \delta$, and hence $T_{11} \leq 2\delta$. Putting all pieces together, we conclude that under the sample complexity $n \geq C_3 \delta^{-2} d \log n$, with probability at least $(1 - \frac{1}{n^9}) \cdot (1 - 2 \exp(-\Omega(d)))$, also exceeding $1 - 2 \exp(-\Omega(d)) - 2n^{-9}$, we have $T \leq C\delta$ for some absolute constant C . The proof is complete. \square

Remark 6. *Lemma 9 plays the same role as Lemma 7.4 in [9], but is more general since it handles $(i, j) = (1, 2)$. The adopted proof strategy may be of independent technical value. Firstly, We point out the technical refinement of a unified treatment to T_{11} (A.3)–(A.4). This avoids several estimates from Chebyshev’s inequality and produces better probability term. Moreover, our argument is by conditioning on \mathcal{A} and more rigorous than [9], which simply assumed \mathcal{A} holds without estimating the expectation error term T_{12} in (A.2).*

B Variants of Quaternion Wirtinger Flow

Two representative refinements for WF are TWF [15] and TAF [62], which enjoy better theoretical guarantee and experimental performance. In this section we present the corresponding algorithms (QTWF, QTAF) for QPR. Just like PQWF, the pure quaternion priori can be similarly incorporated, so we simply focus on a general quaternion signal \mathbf{x} .

B.1 Quaternion Truncated Wirtinger Flow (QTWF)

Following [15], we consider the maximum likelihood estimate under Poisson noise:

$$\max_{\mathbf{z} \in \mathbb{Q}^d} \mathcal{L}(\mathbf{z}) := \frac{1}{n} \sum_{k=1}^n y_k \log(|\mathbf{a}_k^* \mathbf{z}|^2) - |\mathbf{a}_k^* \mathbf{z}|^2.$$

By Chain rule and Table IV in [66], we obtain $\nabla \mathcal{L}(\mathbf{z}) = (\frac{\partial \mathcal{L}}{\partial \mathbf{z}})^* = \frac{1}{2n} \sum_{k=1}^n (\frac{y_k}{|\mathbf{a}_k^* \mathbf{z}|^2} - 1) \mathbf{a}_k \mathbf{a}_k^* \mathbf{z}$, (it would fine that we assume $|\mathbf{a}_k^* \mathbf{z}| > 0$ for all k since the gradient would be trimmed by \mathcal{E}_1 below).

Parallel to Algorithm 1 of [15], under pre-specified parameters $\theta_z^{\text{lb}}, \theta_z^{\text{ub}}, \theta_h, \theta_y$ the spectral initialization is given by $\mathbf{z}_0 = \lambda_0 \cdot \tilde{\mathbf{v}}_{in}$, where $\lambda_0 = (\sum_{k=1}^n y_k/n)^{1/2}$, $\tilde{\mathbf{v}}_{in}$ is the eigenvector corresponding to the largest standard eigenvalue of $\tilde{\mathbf{S}}_{in} = \frac{1}{n} \sum_{k=1}^n y_k \mathbf{a}_k \mathbf{a}_k^* \mathbb{1}_{\{|y_k| \leq \theta_y^2 \lambda_0^2\}}$, which is constructed more selectively compared to \mathbf{S}_{in} in (3.7).

The QWF update is also modified to be more selective by truncation. For the current iteration point \mathbf{z}_t , we let $K_t = \frac{1}{n} \sum_{k=1}^n |y_k - |\mathbf{a}_k^* \mathbf{z}_t|^2|$ and define $\mathcal{E}_1 := \{k : \theta_z^{\text{lb}} \leq \frac{|\mathbf{a}_k^* \mathbf{z}_t|}{\|\mathbf{z}_t\|} \leq \theta_z^{\text{ub}}\}$, $\mathcal{E}_2 := \{k : |y_k - |\mathbf{a}_k^* \mathbf{z}_t|^2| \leq \theta_h K_t \frac{|\mathbf{a}_k^* \mathbf{z}_t|}{\|\mathbf{z}_t\|}\}$. Then, we adopt a QTWF update with step size η and a carefully trimmed gradient reads as

$$\mathbf{z}_{t+1} = \mathbf{z}_t + \frac{\eta}{2n} \sum_{k \in \mathcal{E}_1 \cap \mathcal{E}_2} (\frac{y_k}{|\mathbf{a}_k^* \mathbf{z}_t|^2} - 1) \mathbf{a}_k \mathbf{a}_k^* \mathbf{z}_t.$$

B.2 Quaternion Truncated Amplitude Flow (QTAF)

QTAF is based on the amplitude-based model $y'_k = |\boldsymbol{\alpha}_k^* \mathbf{x}|$ (hence $y'_k = \sqrt{y_k}$), and the goal is to minimize the corresponding ℓ_2 loss

$$\min_{\mathbf{z} \in \mathbb{Q}^d} \ell(\mathbf{z}) := \frac{1}{n} \sum_{k=1}^n (|\boldsymbol{\alpha}_k^* \mathbf{z}| - y'_k)^2.$$

This algorithm adopts the orthogonality-promoting initialization that is radically different from spectral initialization in [9]. Specifically, we pick $\rho \in (0, 1)$ and define $\bar{\mathcal{I}}_0 \subset [n]$ as the indices corresponding to the $\lceil \rho n \rceil$ largest values of $y'_k / \|\boldsymbol{\alpha}_k\|$, and then let $\hat{\mathbf{v}}_{in}$ be the normalized eigenvector corresponding to the largest standard eigenvalue of $\hat{\mathbf{S}}_{in} = \frac{1}{|\bar{\mathcal{I}}_0|} \sum_{k \in \bar{\mathcal{I}}_0} \frac{\boldsymbol{\alpha}_k \boldsymbol{\alpha}_k^*}{\|\boldsymbol{\alpha}_k\|^2}$. Combining a norm estimate, we set $\mathbf{z}_0 = (\sum_{k=1}^n y_k / n)^{1/2} \cdot \hat{\mathbf{v}}_{in}$.

For the update we pick a parameter $\hat{\gamma} > 0$, and for current point \mathbf{z}_t we restrict to the set of indices $\mathcal{I}_{t+1} := \{k \in [n] : |\boldsymbol{\alpha}_k^* \mathbf{z}_t| \geq \frac{1}{1+\hat{\gamma}} y'_k\}$. Note that for $k \in \mathcal{I}_{t+1}$ no ambiguity could arise in the gradient of $(|\boldsymbol{\alpha}_k^* \mathbf{z}| - y'_k)^2$, which is given by $(\frac{\partial}{\partial \mathbf{z}} (|\boldsymbol{\alpha}_k^* \mathbf{z}| - y'_k)^2 \Big|_{\mathbf{z}=\mathbf{z}_t})^* = \frac{1}{2} \boldsymbol{\alpha}_k (\boldsymbol{\alpha}_k^* \mathbf{z}_t - y'_k \frac{\boldsymbol{\alpha}_k^* \mathbf{z}_t}{|\boldsymbol{\alpha}_k^* \mathbf{z}_t|})$. Thus, with step size η , the QTAF update is

$$\mathbf{z}_{t+1} = \mathbf{z}_t - \frac{\eta}{2n} \sum_{k \in \mathcal{I}_{t+1}} \left(1 - \frac{y'_k}{|\boldsymbol{\alpha}_k^* \mathbf{z}_t|}\right) \boldsymbol{\alpha}_k \boldsymbol{\alpha}_k^* \mathbf{z}_t.$$